Synthesis & Characterization of [14]Thiatriphyrin(2.1.1) and Crystallization & Physical Properties of Thiatripyrrine Co-crystals

A thesis submitted towards the partial fulfillment of
BS-MS Dual Degree Programme

by

Rajkumar Yadav
20091066

Under the guidance of
Dr. V.G. Anand
Associate Professor, Chemistry Division,
IISER, Pune

Department of Chemistry
Indian Institute of Science Education and Research, Pune

Certificate

This is to certify that this dissertation entitled **"Synthesis and Characterization of [14]Thiatiphyrin(2.1.1) and Crystallization & Physical Properties of Thiatripyrrine Co-crystals"** towards the partial fulfillment of the BS-MS dual degree programme at the Indian Institute of Science Education and Research, Pune represents original research carried out by **"Rajkumar Yadav at IISER, Pune"** under the supervision of **"Dr. V. G. Anand, Associate Professor, Department of Chemistry"** during the academic year 2013-2014.

Date: Supervisor

Place: Pune (Dr. V. G. Anand)

Declaration

I hereby declare that the matter embodied in the report entitled **"Synthesis and Characterization of [14] Thiatriphyrin(2.1.1) and Crystallization & Physical Properties of Thiatripyrrine Co-crystals"** are the results of the investigations carried out by me at the Department of Chemistry, Indian Institute of Science Education and Research Pune, under the supervision of Dr. V. G. Anand and the same has not been submitted elsewhere for any other degree.

Date: Rajkumar Yadav

Place: Pune

To my beloved family…

Acknowledgments

First and foremost I thank to my guide Dr. V. G. Anand for giving me the opportunity to explore the chemistry that interested me the most at that time when I was in 2nd yr of BS-MS and also for his guidance and freedom to me to carry out research in whatever way I wanted to and how I wanted to. I am thankful to him for a lot of other things, too.
I would like to thank to my advisory committee member Dr. R. Boomi Shankar.

Thanks a lot to Kiran Reddy Baddigam and Dr. M. Jayakannan for their kind and valuable advice in my difficult time during project work.
GopalaKrishna Yadagiri, thanks, for helping me to crank out this thesis through our discussions. Santosh Gadekar, Anant K. Srivastava and Amod, thanks for the many helpful suggestions, too.
I also thank to INSPIRE Programme for financial support and Prof. K. N. Ganesh, Director, IISER Pune for the state-of-art facilities and instrumentations.

Thanks to the following people;
My contemporaries Gopal, Santosh Gadekar, Kiran, Rakesh, Santosh Panchal, Prakhar, Kaushik for their constant help and who made learning enjoyable in the lab.
People in acquiring instrumental data; Archana for X-ray crystallography, Sweta for MALDI-TOF, Naina for HRMS, Pooja and Deepali for NMR.
All the lab mates in Mendleev block for their kind help and making the memories special here.
To my all undergraduate lab friends Vimlesh, Indra, Amrit, Arun, Anurag, Vivek, Rupal, Vikash, Srijit, Venu, Ravi Raja for sharing all good, bad moments, tea parties and meeting sessions at Mendleev Block. I would also like to thank to my friends outside the lab who have helped make my graduate years so enjoyable, includes Sumit, Shibananda, Anurag, Indra, Vivek, Vimlesh, Rupal, Sher, Pramod, Anurag Mishra, Punya, Dhal, Bhavesh, Rohit, Akash, Aditi, Ankita S, Shubham, Raju, Rahul, Suresh, Sharad etc.

Finally I would like to dedicate this work to my family members who have always been the source of support, strength and inspiration throughout my schooling and graduation and for their love from childhood to now. Thank you.

Table of Contents

List of Figures 7

List of Tables 9

Abstract 10

Chapter 1: Synthesis and Characterization of [14]Thiatriphyrin(2.1.1) 11

1.1 Introduction 11

1.2 Synthesis, Results & Discussion 13

1.3 Summary 18

1.4 General Experimental Methods and Techniques 18

1.4.1 Chemicals for Synthesis: 18

1.4.2 Physico-chemical techniques 18

1.4.3 Synthesis of Chemical Compounds 19

1.5 Characterization spectral data: 21

1.6 References 26

Chapter 2: Crystallization and Physical Properties of Thiatripyrrine Co-crystal 29

2.1 Introduction 29

2.2 Preparation, Results and Discussion 31

2.2.1 Thaitripyrrine – DMF co-crystal 31

2.2.2 Thaitripyrrine – Acetonitrile co-crystal 35

2.2.3 Thaitripyrrine – Acetone co-crystal 38

2.3 Summary 45

2.4 Experimental Methods 46

2.4.1 Chemicals for Synthesis: 46

2.4.2 Synthesis of Chemical Compounds 46

2.5 Characterization spectral data: 48

2.6 References 50

List of Figures

Figure 1.1: Chemical Structures of Porphyrin, Corrole and Nor-corrole 11

Figure 1.2: Chemical Structures of Ring-contracted porphyrins 12

Figure 1.3: Chemical Structures of Triphyrin and thiatriphyrin 12

Figure 1.4: Synthetic scheme of diformylthiatripyrrane (5) 13

Figure 1.5: Synthetic scheme of macrocycles 6 and 7 14

Figure 1.6: Synthetic scheme of conjugated macrocycles 8 and 9 14

Figure 1.7: Electronic absorption spectra of macrocycles 8 and 9 15

Figure 1.8: Molecular structure of 17. The top view (above) and the side view (below) 17

Figure 1.9: ^{1}H NMR of 3 21

Figure 1.10: ^{1}H NMR of 4 22

Figure 1.11: ^{1}H NMR of 5 22

Figure 1.12: ^{13}C NMR of 5 23

Figure 1.13: HRMS of 5 23

Figure 1.14: ^{1}H NMR of 8 24

Figure 1.15: ^{1}H-^{1}H COSY of 8 24

Figure1.16: HRMS of 8 25

Figure 1.17: MALDI-TOF mass spectrum of 9 25

Figure 2.1: Chemical structures of quinine, hydroquinone and molecular structure of co-crystal quinhydrone 29

Figure 2.2: Chemical structures of thiatripyrrine (4), DMF, Acetonitrile and Acetone 30

Figure 2.3: Packing diagram of (i) thiatripyrrine-DMF co-crystal, (ii) down the ‘a’ axis, (iii) down the ‘b’ axis 32

Figure 2.4: FTIR spectra of the 1:1 thiatripyrrine : DMF co-crystal 33

Figure 2.5: TGA graph of the 1:1 thiatripyrrine : DMF co-crystal 34

Figure 2.6: UV-Visible spectra of thiatripyrrine-DMF co-crystal in (i) DCM, (ii) CHCl3 and (iii) Ethyl acetate 35

Figure 2.7: (i) conformation of free thiatripyrrine, (ii) conformation of thiatripyrrine in co-crystal 35

Figure 2.8: Packing diagram of (i) thiatripyrrine-Acetonitrile co-crystal, (ii) down the 'a' axis, (iii) down the 'b' axis 36

Figure 2.9: FTIR spectra of the 1:1 thiatripyrrine : acetonitrile co-crystal 37

Figure 2.10: TGA graph of the 1:1 thiatripyrrine : Acetonitrile co-crystal 38

Figure 2.11: Packing diagram of (i) thiatripyrrine-acetone co-crystal, (ii) down the 'a' axis, (iii) down the 'b' axis 39

Figure 2.12: FTIR spectra of the 1:1 thiatripyrrine : Acetone co-crystal 40

Figure 2.13: TGA graph of the 1:1 thiatripyrrine : Acetone co-crystal 41

Figure 2.14: Chemical structures of 2,2'-(phenylmethylene)bis(1H-pyrrole) and 5,5'-bis(phenyl(1H-pyrrol-2-yl)methyl)-2,2'-bithiophene 43

Figure 2.15: Crystal structures of (i) 2,2'-(phenylmethylene)bis(1H-pyrrole), (ii) 5,5'-bis(phenyl(1H-pyrrol-2-yl)methyl)-2,2'-bithiophene 43

Figure 2.16: Total energy profile of thiatripyrrine conformations 44

Figure 2.17: Optimized geometry of free tripyrrine showing dihedral angle 45

Figure 2.18: Synthetic scheme of compound 11 45

Figure 2.19: ^{1}H NMR of 10 48

Figure 2.20: ^{1}H NMR of 13 49

Figure 2.21: ^{1}H NMR of 12 49

Figure 2.22: ^{1}H NMR of 11 50

List of Tables

Table 1.1: Crystallographic data for macrocycle 8 17

Table 2.1: Hydrogen bond geometry in thiatripyrrine-DMF co-crystal 33

Table 2.2: Hydrogen bond geometry in thiatripyrrine-acetonitrile co-crystal 37

Table 2.3: Hydrogen bond geometry in thiatripyrrine-acetone co-crystal 40

Table 2.4: Crystallographic data for thiatripyrrine co-crystals 42

Abstract

In chapter 1 of the thesis, a thiophene containing triphyrin called [14] Thiatriphyrin(2.1.1) was synthesized by McMurry coupling of diformylthiatripyrrane followed by oxidation with p-chloranil. This was characterized by MALDI-TOF, HRMS, UV-Visible, ^{1}H NMR, ^{1}H-^{1}H COSY and Single Crystal XRD spectroscopic techniques. These thiatriphyrins have a 14π-electron pathway and have non-planar structure probably due to the larger size of sulphur atom compared to inner nitrogen atoms and electronic repulsion between the lone pairs of nitrogen atoms.

In chapter 2 of the thesis, the work focuses on the crystallization and physical properties of the thiatripyrrine co-crystals. Co-crystals of thiatripyrrine with dimethylformamide (DMF), acetonitrile and acetone have been examined. These co-crystals have been successfully prepared by dissolving thiatripyrrine in these molecules (used as solvent) and by passing the resulting solution through a syringe resulted in immediate nucleation. By varying the amount of thiatripyrrine and type of syringe, yield and productivity can be significantly increased. Single crystal X-ray diffraction was used to identify the 1:1 molar ratio of the parent compounds in the co-crystal. UV-Visible spectroscopy was used to check the reversibility of thiatripyrrine conformation in different solvents. The disintegration temperatures of co-crystals were determined by TGA and melting point. The formation of hydrogen bonds in thiatripyrrine co-crystals were investigated by FTIR. Computational studies were carried out to estimate the optimization energy of free thiatripyrrine conformation, the thiatripyrrine conformation in co-crystal and its other conformations along the dihedral angle.

Chapter 1: Synthesis and Characterization of [14]Thiatriphyrin(2.1.1)

1.1 Introduction

Porphyrins are well known and are a group of naturally occurring organic compounds in proteins and enzymes such as hemoglobin, myoglobin, chlorophyls, cytochromes etc. These are heterocyclic macrocycles consisting of four pyrrole subunits linked by four methine bridges (=CH-) (Figure 1.1). These porphyrins are employed in various areas; complexes of their metal ion can catalyze a variety of reactions in organic synthesis, in medicine; they find application in molecular degeneration using verteporfins[1], in molecular electronics; as photovoltaic devices[2] [3], in supramolecular chemistry; as a host-guest complex due to macrocyclic cavity[4]. Ring-contracted porphyrins are a series of porphyrinoids, which either lack meso carbons or one of the four pyrroles. Corroles are tetrapyrrolic macrocycles which lack one methine carbon from porphyrins (Figure 1.1) and have one direct pyrrole-pyrrole link. They can be used as ligands which can stabilize high valence metal ions. Nor-corroles are also tetrapyrrolic macrocycles which lacks two methine carbons compared to parent porphyrins and have two direct pyrrole-pyrrole links (Figure 1.1). These macrocycles display anti-aromatic character with 16π-electrons[5].

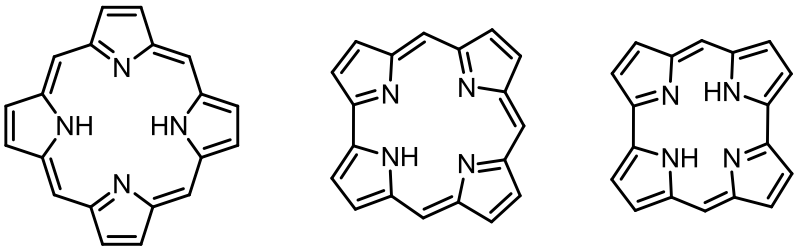

Figure 1.1: Chemical Structures of Porphyrin, Corrole and Nor-corrole

Triphyrins are a subclass of modified porphyrins and are described by a general formula [N]triphyrin(x.y.z) where N is the sum of macrocyclic π-electrons and x,y,z are the number of linker atoms between the heterocycles[6]. Triphyrin is a tripyrrolic macrocycle lacking one pyrrole and one meso carbon from the parent porphyrin framework (figure 1.2). In the recent years, there has been enough report on the ring-expanded porphyrinoids but the chemistry of ring-contracted porphyrinoids is relatively new. The first triphyrin-related compound was reported in 1972 as subthalocynine[7] prepared from pthalonitrile in the presence of BCl_3 and the next,

subporphyrazine, was reported only in 2005[8] (Figure 1.2). In 2006, Osuka et al. reported the tribenzosubporphyrin ([14]benzotriphyrin(1.1.1))[9] replacing all nitrogen atoms at the meso-position of subphtalocyanine by methine carbons and subsequently they developed synthetic protocols for meso-aryl substituted subporphyrins[10] [11] (Figure 1.2).

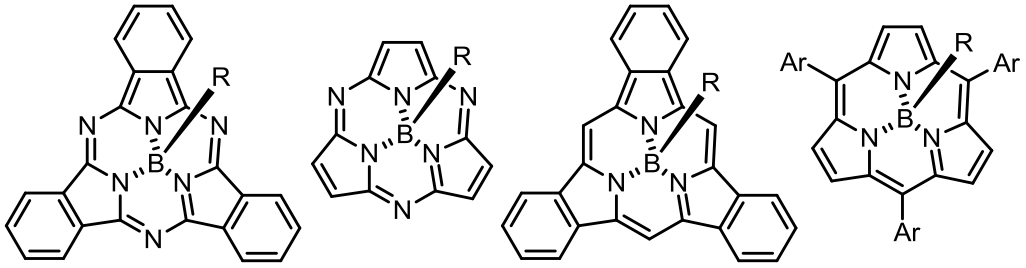

Figure 1.2: Chemical Structures of Ring-contracted porphyrins

These subporphyrins display strong fluorescence properties and its emission can be tuned by their meso-substituents. These triphyrins have demonstrated a variety of optoelectronic properties in high technology fields such as non-linear optical absorption [12], highly fluorescent compounds and high emission quantum yield [13] and have been applied in organic devices, such as organic light-emitting diodes (OLED) [14] and organic solar cells (OSC) [15]. In 2008, [14]triphyrin(2.1.1) was reported which has near-planar structure and having a 14π-electron aromatic pathway composed of only pyrrole moieties and since they are boron-free triphyrin, they can be converted into bowl-shaped Mn^{I}, Re^{I}, and Ru^{II} complexes [16] (Figure 1.3) and work as monoanionic-tridentate ligands.

Figure 1.3: Chemical Structures of Triphyrin and thiatriphyrin

It is well known that the core modifications of these porphyrinoids cause phenomenal alterations in the optical, electrochemical properties and its coordination abilities [17]. Since [14]triphyrins(2.1.1) frameworks are flexible and suitable to many metal ions, so it can be expected that core modification of these triphyrins would also result in

phenomenal changes in its optical, electrochemical properties etc. Hence we decided to synthesize thiatriphyrin and explore its properties.

1.2 Synthesis, Results & Discussion

The thiatriphyrin was synthesized by the intramolecular McMurry coupling of diformylthiatripyrrane. It was explored by Uno and co-workers [18] in their attempt to synthesize triphyrin. Thiophene **1** was lithiated with n-BuLi to give lithiated solution **2** which was further reacted with benzaldehyde to give its diol **3**. Thiophenediol **3** was then reacted to pyrrole (in excess) in the acidic condition to give thiatripyrrine **4**. The diformylthiatripyrrane **5** was synthesized by Vilsmeir reaction, reacting thiatripyrrine **4** with Vilsmeir product formed by $POCl_3$ in DMF (excess), in good yield (Figure 1.4).

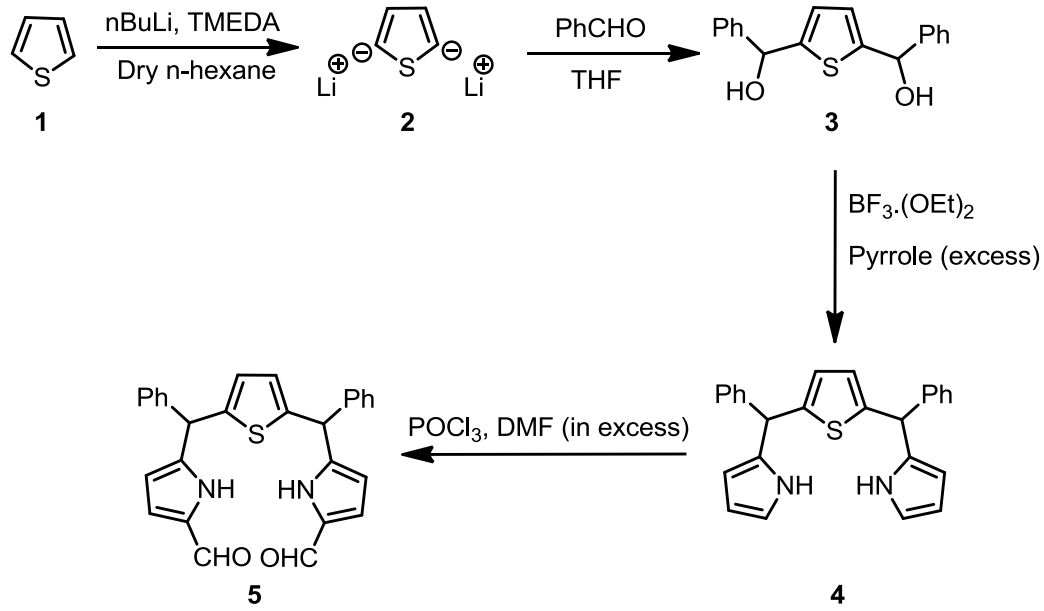

Figure 1.4: Synthetic scheme of diformylthiatripyrrane (**5**)

The diformylthiatripyrrane **5** was subjected to intramolecular McMurry coupling under inert condition resulted in unconjugated macrocycles as described in figure 1.5.

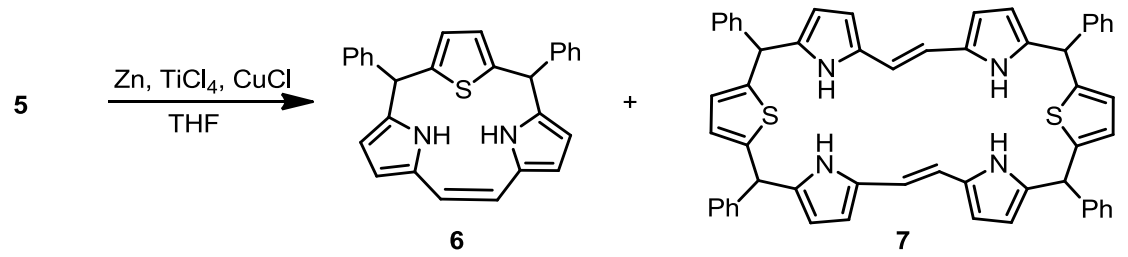

Figure 1.5: Synthetic scheme of macrocycles 6 and 7

These products could be detected in the MALDI-TOF mass spectrum of the reaction mixture. The reaction mixture was passed through basic alumina to get unconjugated macrocycles **6** and **7**. They were further oxidized by *p*-chloranil in CH_2Cl_2 to obtain the conjugated macrocycles as described in figure 1.6.

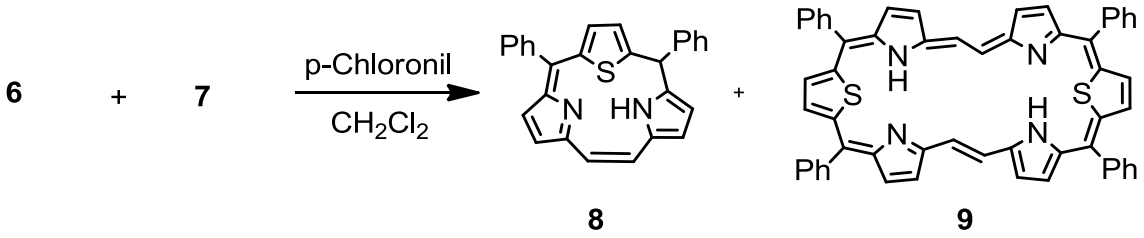

Figure 1.6: Synthetic scheme of conjugated macrocycles 8 and 9

These conjugated macrocycles could be detected in MALDI-TOF mass spectrum in the reaction mixture and the reaction mixture was purified by column chromatography to isolate the macrocyclic products **8** and **9**. 8 was isolated in good yield (30%) while the macrocyclic product **9** was isolated in poor yield. In order to increase the yield of the bigger macrocycle, we subjected the same reaction under concentrated conditions.

Macrocycle **8** named [14]thiatriphyrin(2.1.1) was characterized by various analytical techniques before arriving at the final structure of the macrocycle while the complete characterization of macrocycle **9** is in progress. The molecular mass of macrocycle **8** was confirmed by HRMS mass spectrometric analyses, showed m/z value at 417.1489 against its calculated value at 417.1423 $(M+H)^+$. The molecular mass of **9** was confirmed by MALDI-TOF mass spectrometric analyses. It displayed m/z value at 830.2370 against its calculated value at 830.2538.

Due to their extended conjugation system, they form colored solutions in organic solvents and absorb in visible region of the electromagnetic spectrum (Figure 1.7). Thiatriphyrin **8** accounts for 14π-electron along its conjugated pathway and has four

absorption bands at 260, 308, 401 and 535 nm, whereas **9** displayed its four absorption bands at 278, 323, 406 and 559 nm.

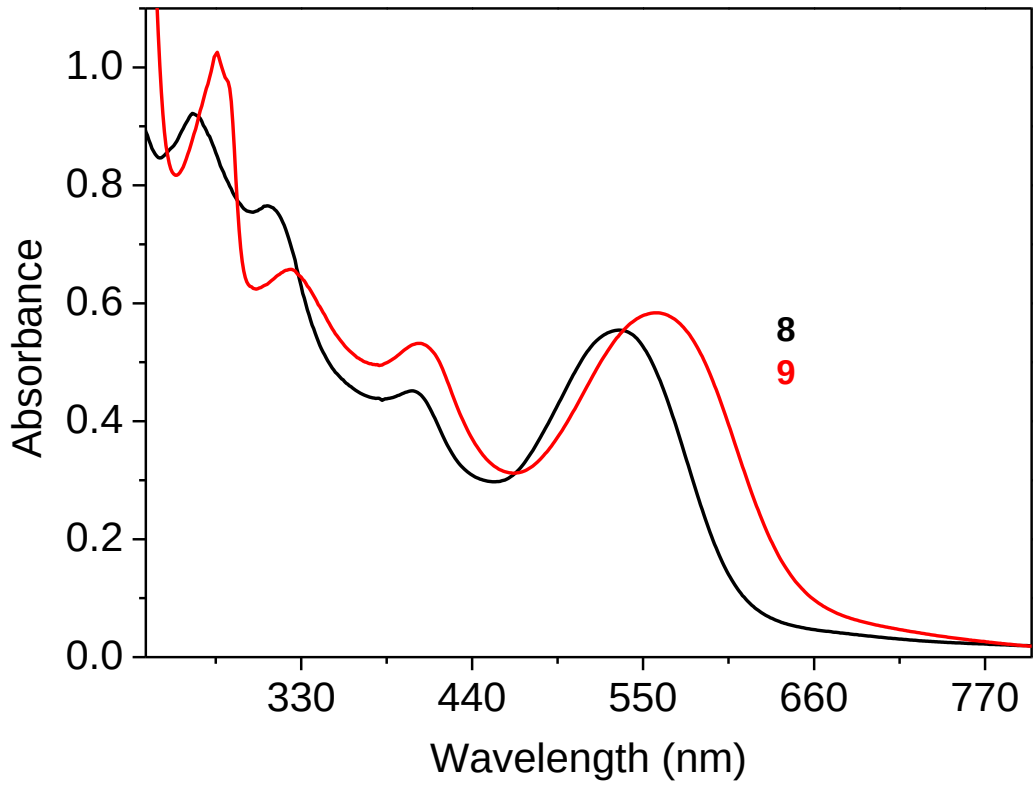

Figure 1.7: Electronic absorption spectra of macrocycles **8** and **9**

These macrocycles were also further characterized by ^{1}H NMR to determine their structure in solution state. ^{1}H NMR of Thiatriphyrin **8** shows a resolved spectrum in $CDCl_3$ at room temperature exhibiting doublet at δ 6.15, triplet at δ 6.19, doublet at δ 6.26, triplet at δ 6.65, doublet at δ 6.84, multiplet at δ 6.90, multiplet at δ 7.41, multiplet at δ 7.47, doublet at 7.70, doublet of doublet at δ 7.79 and broad NH peak at δ 13.07.

We attempted to grow single crystals of these macrocycles to determine the absolute conformation in solid state. Good quality crystals suitable for X-ray diffraction analysis were obtained for macrocycle **8** (thiatriphyrin) by the slow evaporation of methanol/hexane. Since the meso-carbon hydrogen of macrocycle **8** is much reactive. Its reaction with methanol during crystallization was confirmed from its crystal structure. The methoxy group at the meso carbon is oriented in the same direction as the sulphur atom relative to the plane of the macrocycle (Figure 1.8).

The bond length (C-N) in the pyrrole moieties indicates that one pyrrole unit has the structure of imine whereas other pyrrole unit has the structure of amine and the N···N (D···A) distance was found to be 2.716Å, and 1.958Å for H···N (H···A). This suggests intramolecular hydrogen bonding interaction between the two nitrogen atoms as their distances among hydrogen, donor and acceptor follow the geometrical criteria for hydrogen bonding (D-A < 3.9Å, H-A < 2.5Å). The thiophene ring is significantly tilted out of the plane of the macrocycle probably because of the large size of thiophene atom compared to nitrogen atoms and electronic repulsion between the two lone pairs of the inner nitrogen atoms. Steric repulsion between the large sulphur atom and the two electron lone pairs of the nitrogen atoms in the small cavity make the thiatriphyrin molecule non-planar and reduce the aromatic stability.

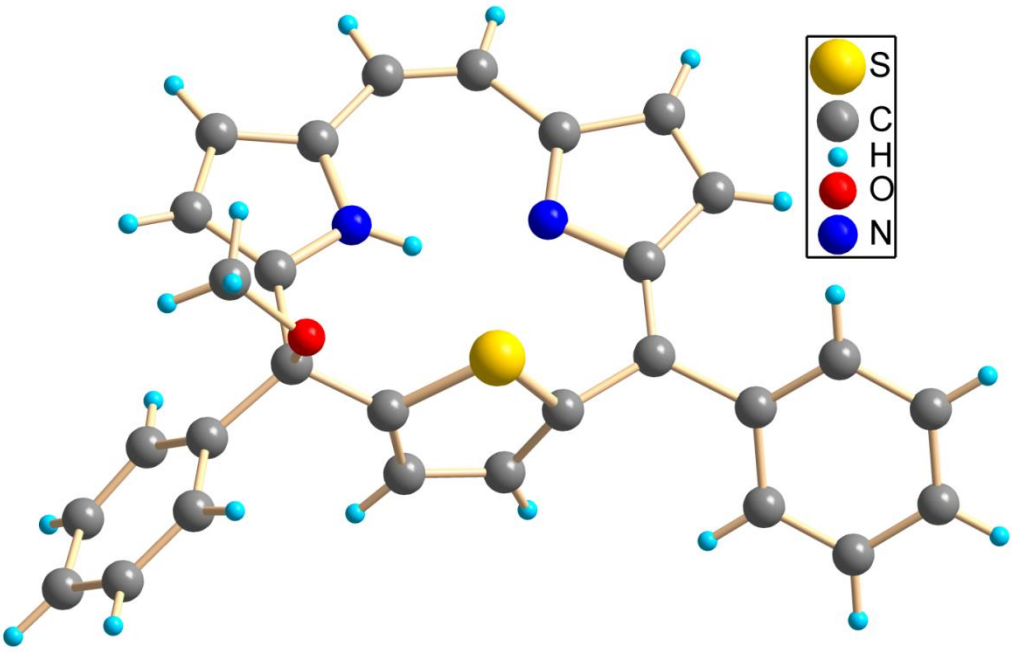

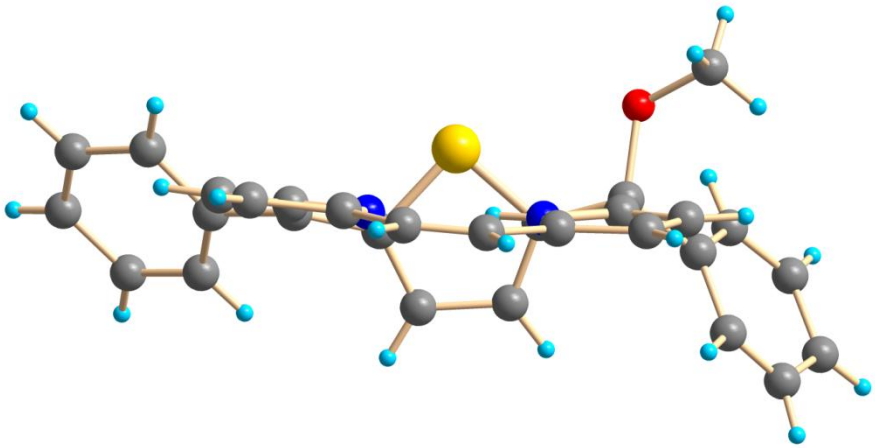

Figure 1.8: Molecular structure of 17. The top view (above) and the side view (below)

Macrocycle	**8**
Solvent system	Methanol/Hexane
Chemical formula	$C_{29}H_{22}N_2SO$
M (g mol^{-1})	446.15
T (K)	100
Crystal system	Triclinic
Space group	P-1
a (Å)	8.9746(13)
b (Å)	13.3832(19)
c (Å)	19.154(3)
α (°)	77.253(3)
β (°)	78.141(3)
γ (°)	76.668(3)
V ($Å^3$)	2154.65
Z/Z'	2/0
R1	0.0972

Table 1.1: Crystallographic data for macrocycle **8**

1.3 Summary

In this chapter, we have featured the synthesis, structure and properties of the new class of ring-contracted porphyrin, [14]thiatriphyrin(2.1.1) in the solid state and solution state. This macrocycle was found to be non-planar due to large size of sulphur atom compared to nitrogen atom and the electronic repulsion between lone pairs of inner nitrogen atoms. Further synthesis of its metal complexes and core modified triphyrins will be possible and various properties and functions are remained to be explored. Research is underway to synthesize macrocycle **9** in good yield and to complete the characterization.

1.4 General Experimental Methods and Techniques

1.4.1 Chemicals for Synthesis:

Common solvents used for synthesis were purified and dried according to known procedures. Thiophene, pyrrole and benzaldehyde were distilled before use. TMEDA, $BF_3.(OEt)_2$ were used from Aldrich chemicals, USA. n-Butyllithium (1.6M in hexane) was used from E. Merck, Germany. Pyrrole, Benzaldehyde, $POCl_3$, Zn, $TiCl_4$, *p*-chloranil were used from Spectrochem chemicals, India. Thiophene, anhydrous potassium carbonate, anhydrous sodium sulphate, and anhydrous calcium chloride were obtained from Rankem Fine chemicals, India.

1.4.2 Physico-chemical techniques

Electronic spectra were recorded on a Perkin Elmer-Lambda 20 UV-Vis spectrophotometer. The data analyses were done using the UV-winlab software package. ^{1}H and ^{13}C NMR spectra were obtained either from 500 MHz Bruker Advance DPX spectrometer or 400 MHz Jeol machine in $CDCl_3$ using tetramethylsilane (TMS) as integral standard. ESI HRMS data were recorded on Waters Synapt G2 spectrometer. MALDI-TOF was carried out on Voyager-De-STR

(Applied Biosystems). Single crystals were diffracted on Bruker Apex Duo single crystal X-ray diffractometer. The data was solved using Apex-2 software.

1.4.3 Synthesis of Chemical Compounds

Thiophene-2,5-diylbis(phenylmethanol) (3)

Thiophene (1.9 ml, 2.1 gm, 0.025 mol) was added slowly via a syringe to a solution of n-BuLi (39 ml of 1.6M solution in hexane) and tetramethylethylenediamine (TMEDA) (7.5 ml) in 100 ml of dry hexane under an argon atmosphere. The resulting solution was warmed to reflux for 1 hr, cooled to ambient temperature. This dilithiothiophene solution was added slowly to a solution of benzaldehyde (6.15 g, 0.058 mol) in 1 lit of dry THF cooled to 0° C in an ice bath. The ice bath was removed after addition and the reaction was warmed to ambient temperature. The reaction was quenched by a cold, saturated NH_4Cl solution (200 ml) and the organic layer was separated, dried over Na_2SO_4 and concentrated. The desired compound was isolated via column chromatography on silica gel eluted with ethyl acetate/hexane (20:80). The product was collected as white powder (yield: 85%). ^{1}H NMR (400 MHz, $CDCl_3$) δ 7.43 – 7.30 (m, 10H), δ 6.69 (s, 2H), δ 5.96 (s, 2H), δ 2.43 (brs, 2H).

2,5-bis(phenyl(1H-pyrrol-2-yl)methyl)thiophene (4)

Compound **3** (0.5 g, 0.00168 mol) was dissolved in excess pyrrole (4.47 ml) and argon was bubbled through it. $BF_3(OEt)_2$ (0.04 ml) was added and the resulting mixture was allowed to stir for 1 hr. The reaction was quenched by the addition of dichloromethane (50 ml) followed by 40% NaOH (15 ml). The Organic layer was separated, washed with water and brine, dried over sodium sulphate and concentrated under reduced pressure. The residual oil was purified via chromatography on silica gel eluted with ethyl acetate/hexane (5:95). The desired product was collected as yellow oil (yield: 90%). ^{1}H NMR (400 MHz, $CDCl_3$) δ 7.93 (brs, 2H), δ 7.36 – 7.26 (m, 10H), δ 6.71 (s, 2H), δ 6.64 (s, 2H), δ 6.16 (s, 2H), δ 5.95 (s, 2H), δ 5.59 (s, 2H).

5,5'-(thiophene-2,5-diylbis(phenylmethylene))bis(1H-pyrrole-2-carbaldehyde) (5)

In a round bottom flask cooled to 0° C, DMF (0.22 ml, 2.778 mmol) was added. After 10 minutes $POCl_3$ (0.26 ml, 2.778 mmol) was slowly added and orange phosphorescence solution was observed. After 30 minutes, the solution was heated to 60° C and solution became reddish in color. Compound **4** (.5 g, 1.2673 mmol) dissolved in DMF was slowly added to the solution. The resulting mixture was refluxed for 1.5 hrs and then brought to ambient temperature. The reaction was stopped by addition of solution of saturated sodium acetate. The organic layer was separated and dried over Na_2SO_4 and concentrated under reduced pressure. The residue was separated via column chromatography on silica gel eluted with ethyl acetate/hexane (30:70). The desired product was collected as reddish solid (yield: 62%). ^{1}H NMR (400 MHz, $CDCl_3$) δ 9.40 (s, 2H), δ 9.07 (brs, 2NH), δ 7.34 – 7.21 (m, 10H), δ 6.89 (t, J = 4 Hz, 2H), δ 6.63 (s, 2H), δ 6.09 (t, J = 4 Hz, 2H), δ 5.59 (s, 2H).
HRMS: $C_{28}H_{22}N_2O_2S$; 450.1402 (100 %), observed 451.1478 (M+H) (100 %)

Synthesis of 6 and 7

To a mixture of Zn dust (3.5 g) and CuCl (0.20 g, 2.0 mmol) in THF (100 ml) $TiCl_4$ (3.3 ml, 30 mmol) was carefully added and argon was bubbled through it. The resulting black slurry was refluxed for 2 hrs. A solution of compound **5** (0.50 g, 1.0 mmol) in THF (100 ml) was added drop wise to the black slurry and the resulting mixture was refluxed for another 1 hr. The reaction mixture was cooled to 0°C and quenched by the addition of 10% aqueous K_2CO_3 (100 ml). The organic phase was extracted in CH_2Cl_2, washed with water and concentrated under reduced pressure. A mixture of macrocycles **6** and **7** were isolated via column chromatography on basic alumina. They were further oxidized by *p*-chloranil to give macrocycles **8** and **9** which were isolated via column chromatography on basic alumina eluted with CH_2Cl_2/hexane yielded in 30% and around 5-10%.

Data for **8**: ^{1}H NMR (400 MHz, $CDCl_3$) δ 13.07 (brs, 1NH), δ 7.79 (d, J = 8 Hz, 2H), δ 7.70 (d, J = 8 Hz, 2H), δ 7.49 – 7.36 (m, 8H), δ 6.90 (m, 2H), δ 6.84 (d, J = 4 Hz, 1 H), δ 6.65 (m, 1H), δ 6.26 (d, J = 12 Hz, 1H), δ 6.19 (m, 1H), δ 6.15 (d, J = 4 Hz, 1H)
HRMS: $C_{28}H_{20}N_2S$; 416.1423 (100 %), observed 417.1489 (M+H) (100 %)

UV-vis (CH_2Cl_2): λ_{max} (ε [$M^{-1}cm^{-1}$]) 260 nm (3484.9), 308 nm (2894.9), 401 nm (1707.9), 535 nm (2097.5)

Data for **9**: MALDI-TOF: $C_{56}H_{38}N_4S_2$; 830.25 (100%), observed 830.24 (100 %)
UV-vis (CH_2Cl_2): λ_{max} (ε [$M^{-1}cm^{-1}$]) 323 nm (6063.5), 406 nm (4905.7), 559 nm (5385.3)

1.5 Characterization spectral data:

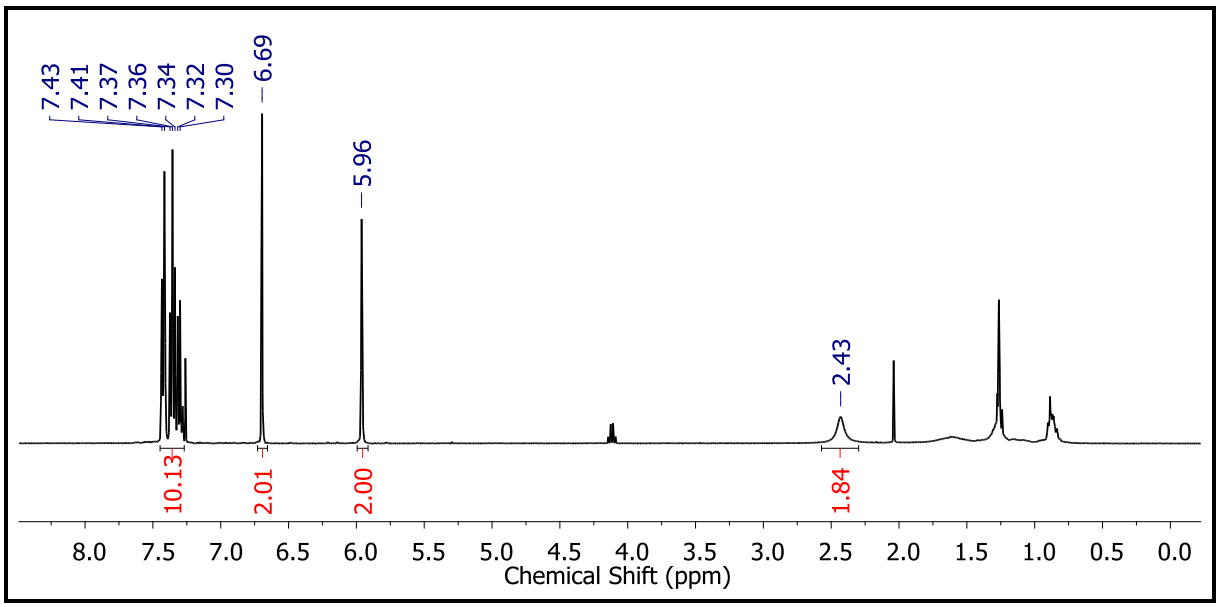

Figure 1.9: ^{1}H NMR of **3**

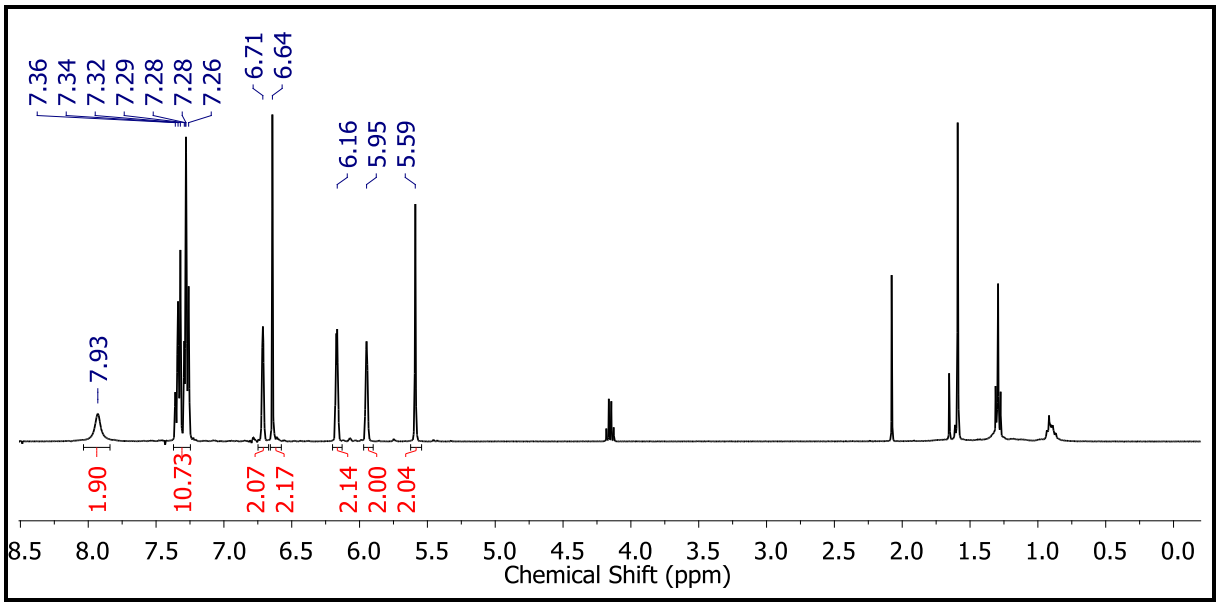

Figure 1.10: ^{1}H NMR of **4**

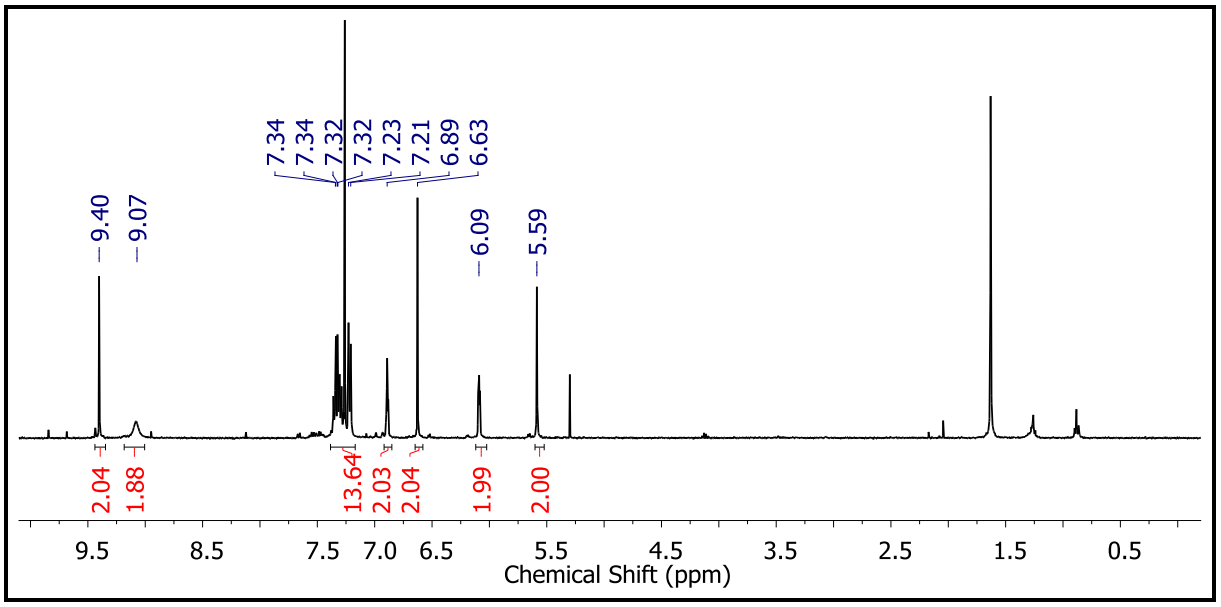

Figure 1.11: ^{1}H NMR of **5**

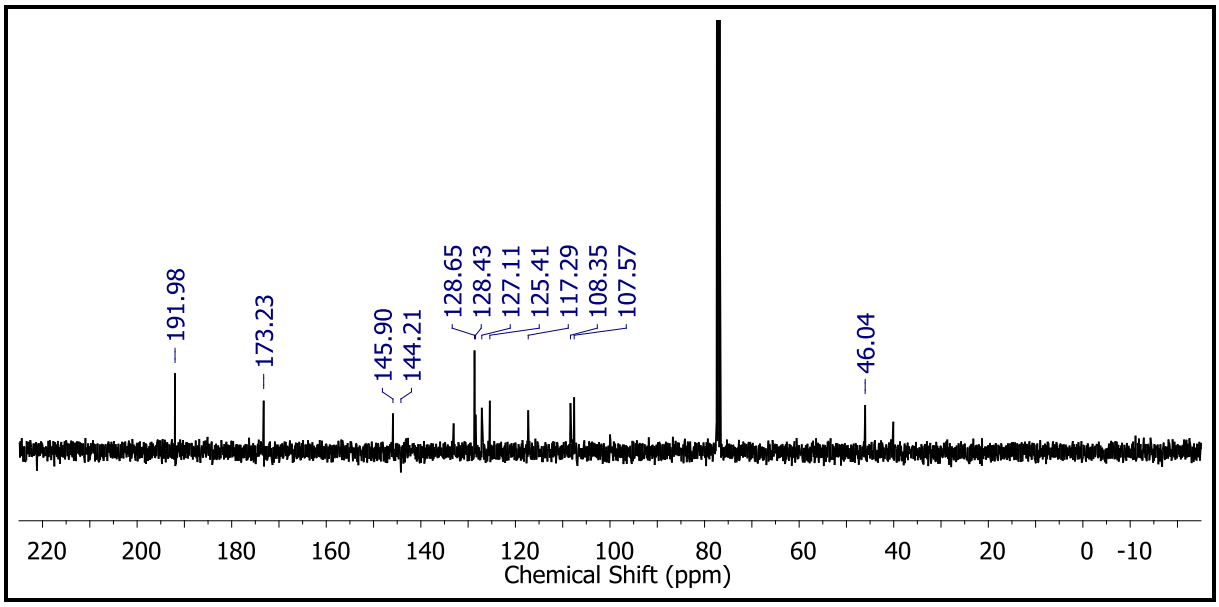

Figure 1.12: ^{13}C NMR of **5**

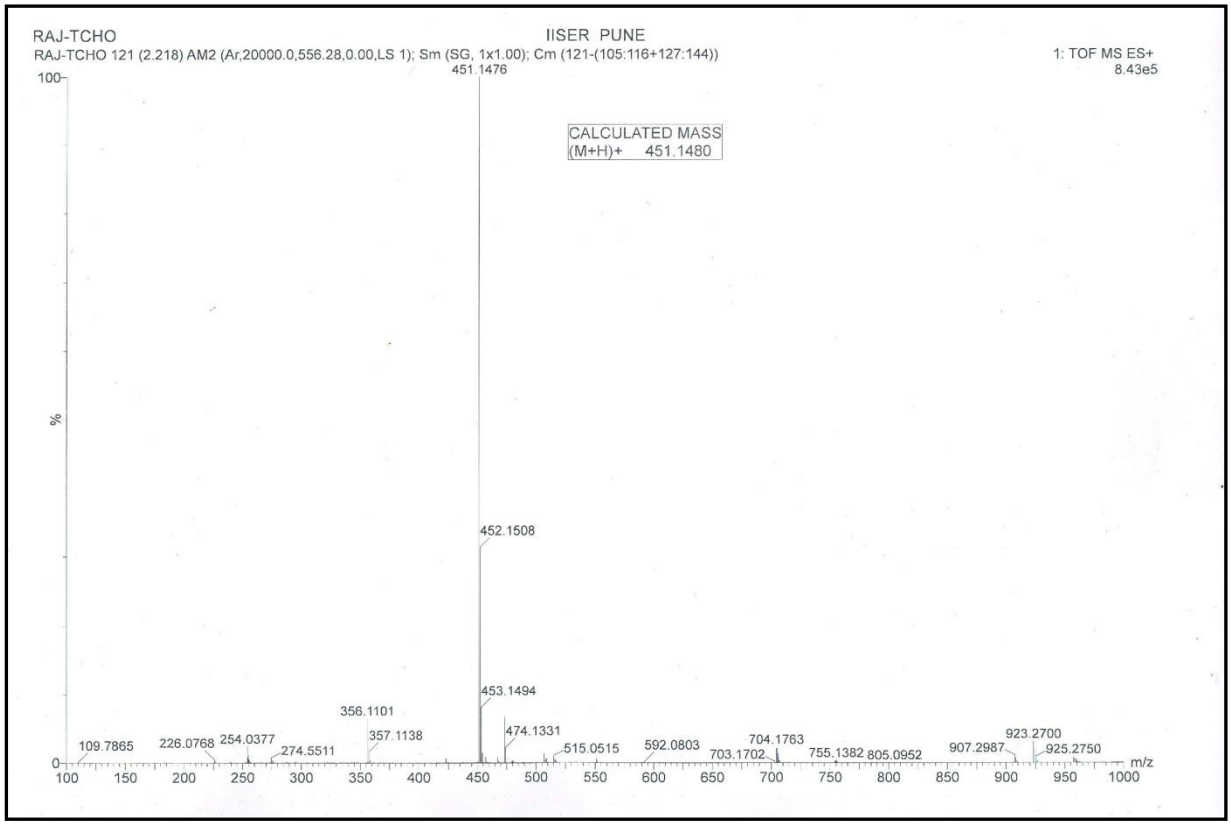

Figure 1.13: HRMS of **5**

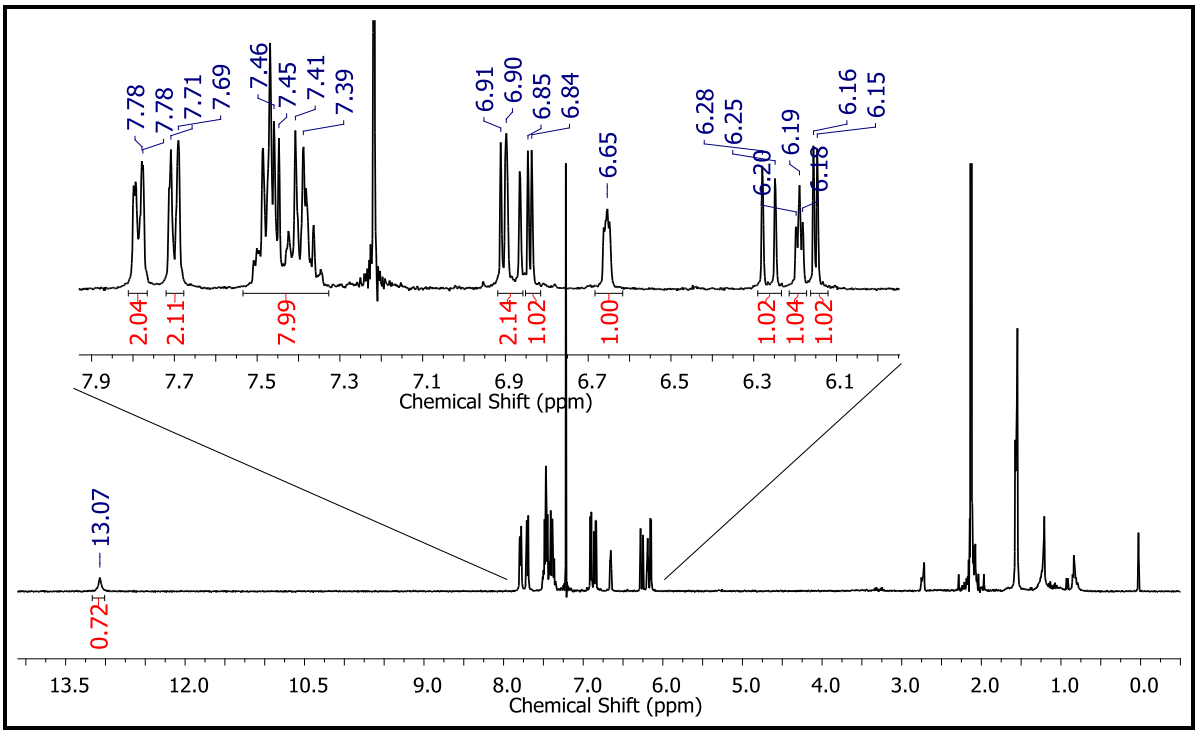

Figure 1.14: ^{1}H NMR of **8**

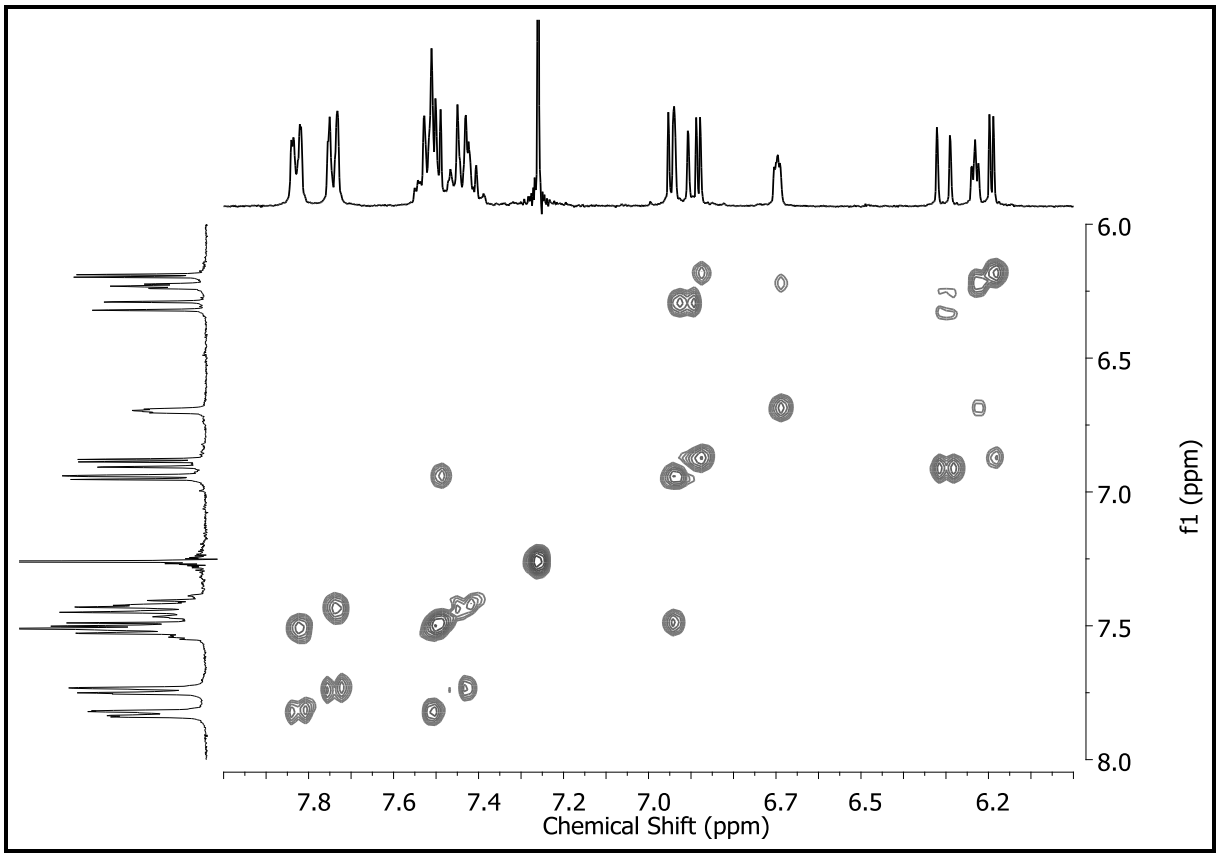

Figure 1.15: ^{1}H-^{1}H COSY of **8**

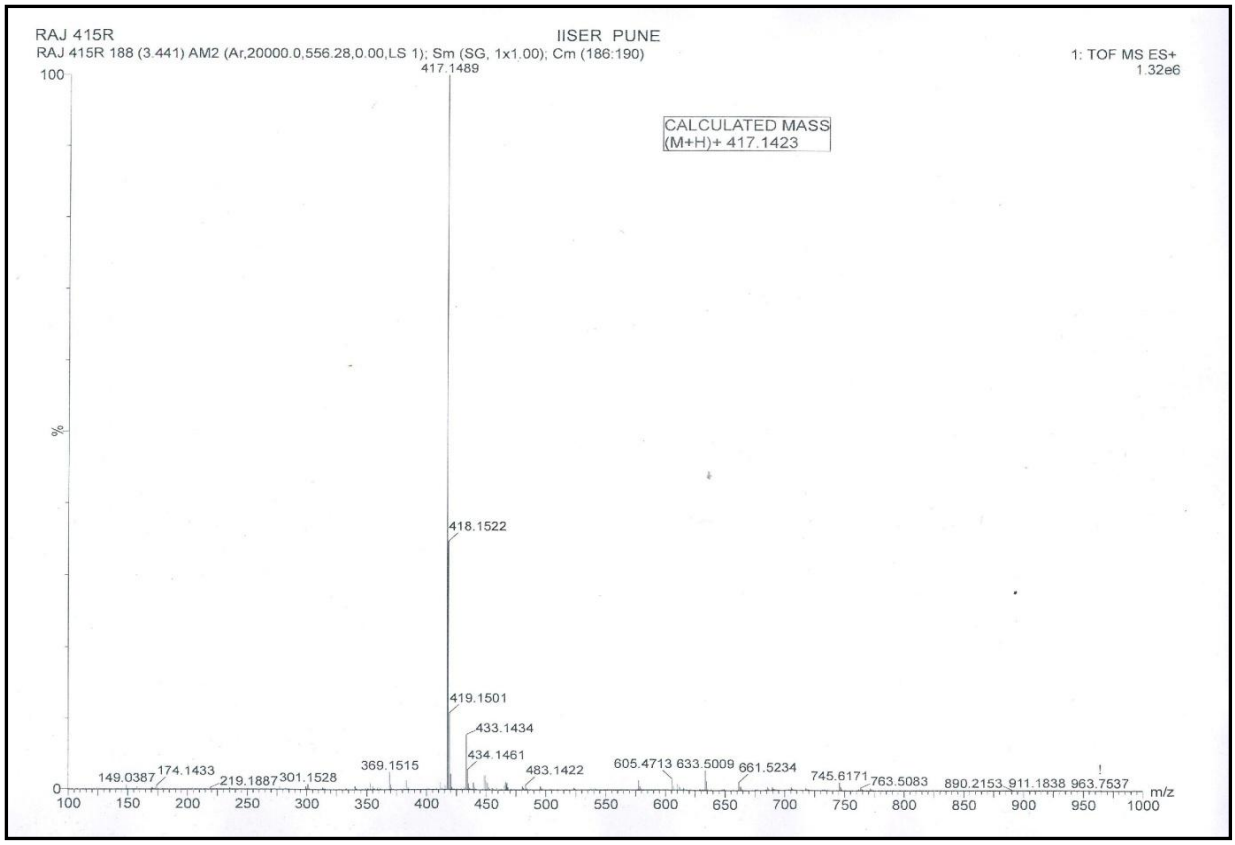

Figure1.16: HRMS of **8**

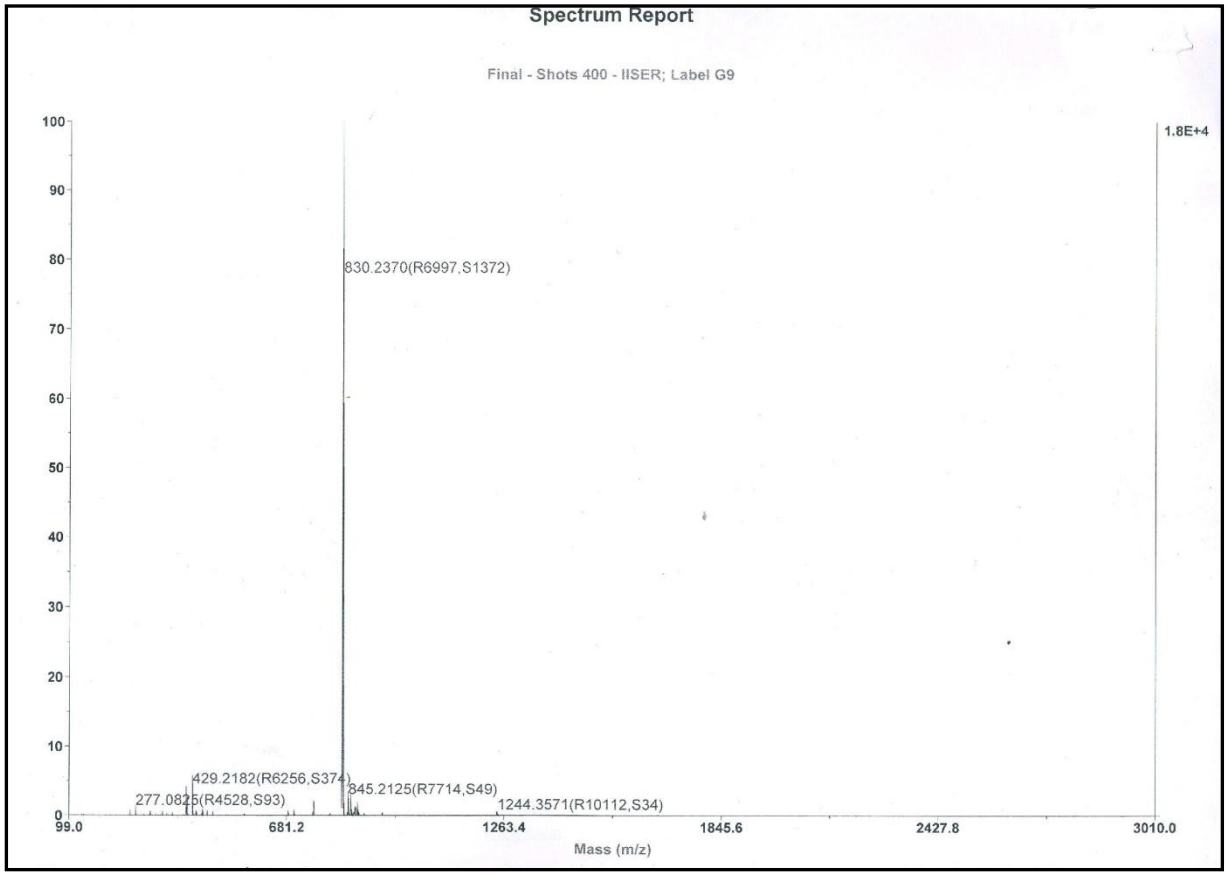

Figure 1.17: MALDI-TOF mass spectrum of **9**

1.6 References

1. Wormald, R; Evans, J; Smeeth, L; Henshaw, K. Photodynamic therapy for neovascular age-related macular degeneration. *Cochrane Database Syst Rev* **2007**, 3, CD002030.
2. Walter, G; Alexander, B; Rudine, C; Wamser. Porphyrins and phthalocyanines in solar photovoltaic cells. *Journal of Porphyrins and Phthalocyanines*, **2010**, 14 (9), 759–792.
3. Yella, A; Lee, H; Tsao, H; Yi, C; Chandiran, A; Nazeeruddin, M; Diau, E; Yeh, C; Zakeeruddin, S; Grätzel, M. Porphyrin-Sensitized Solar Cells with Cobalt (II/III)–Based Redox Electrolyte Exceed 12 Percent Efficiency. *Science*, **2011**, 334 (6056), 629–634.
4. Anderson, S; Anderson, H; Bashall, A; McPartlin, M; Sanders, J. Assembly and Crystal Structure of a Photoactive Array of Five Porphyrins. *Angew. Chem. Int. Ed. Engl*, **1995**, 34 (10), 1096–1099.
5. a) Ghosh, A; Wasbotten, I; Davis, W; Swarts, J. Norcorrole and Dihydronorcorrole: A Predictive Quantum Chemical Study. *Eur. J. Inorg. Chem.*, **2005**, 4479; b) Bröring, M; Köhler, S; Kleeberg, C. Norcorrole: Observation of the Smallest Porphyrin Variant with a N_4 Core. *Angew. Chem. Int. Ed.*, **2008**, 47, 5658; c) Ito, T; Hayashi, Y; Shimizu, S; Shin, J; Kobayashi, N; Shinokubo, H. Gram-Scale Synthesis of Nickel(II) Norcorrole: The Smallest Antiaromatic Porphyrinoid. *Angew. Chem. Int. Ed.*, **2012**, 51, 8542.
6. Kuzuhara, D; Yamada, H. Synthesis and Characterization of Triphyrins: A New Family of Porphyrinoids. *Heterocycles*, **2013**, 87, 6.
7. Meller, A; Ossko, A. Phthalocyaninartige Bor-Komplexe. *Monatsh. Chem*., **1972**, 103, 150.
8. Rodríguez-Morgade, M; Esperanza, S; Torres, T; Barberá, J. Synthesis, Characterization, and Properties of Subporphyrazines: A New Class of Nonplanar, Aromatic Macrocycles with Absorption in the Green Region. *Chem. Eur. J*., **2005**, 11, 354.
9. Inokuma, Y; Kwon, J; Ahn, T; Yoo, M; Kim, D; Osuka, A. Tribenzosubporphines: Synthesis and Characterization. *Angew. Chem. Int. Ed.*, **2006**, 45, 961.

10. Inokuma, Y; Yoon, Z; Kim, D; Osuka, A. *meso*-Aryl-Substituted Subporphyrins: Synthesis, Structures, and Large Substituent Effects on Their Electronic Properties. *J. Am. Chem. Soc.,* **2007**, 129, 4747.
11. Kobayashi, N; Takeuchi, Y; Matsuda, A. *meso*-Aryl Subporphyrins. *Angew. Chem. Int. Ed.*, **2007**, 46, 758.
12. a) Rey, B; Keller, U; Torres, T; Rojo, G; Agull_-L_pez, F; Nonell, S; Mart, C; Brasselet, S; Ledoux, I; Zyss, J. Synthesis and Nonlinear Optical, Photophysical, and Electrochemical Properties of Subphthalocyanines. *J. Am. Chem. Soc.* **1998**, 120, 12808-12817; b) Tsurumaki, E; Inokuma, Y; Easwaramoorthi, S; Lim, J; Kim, D; Osuka, A. Peripheral Hexabromination, Hexaphenylation, and Hexaethynylation of *meso*-Aryl-Substituted Subporphyrins. *Chem. Eur. J.* **2009**, 15, 237 – 247.
13. a) Easwaramoorthi, S; Shin, J; Cho, S; Kim, P; Inokuma, Y; Tsurumaki, E; Osuka, A; Kim, D. Versatile Photophysical Properties of *meso*-Aryl-Substituted Subporphyrins: Dipolar and Octupolar Charge-Transfer Interactions. *Chem. Eur. J.* **2009**, 15, 12005-12017; b) Inokuma, Y; Easwaramoorthi, S; Jang, Y; Kim, S; Kim, D; Osuka, A. Monovalent and Bivalent Fibrin-specific MRI Contrast Agents for Detection of Thrombus. *Angew. Chem. Int. Ed.* **2008**, 120, 4918-4921; Inokuma, Y; Easwaramoorthi, S; Jang, Y; Kim, K; Kim, D; Osuka, A. Effective Expansion of the Subporphyrin Chromophore Through Conjugation with *meso*-Oligo(1,4-phenyleneethynylene) Substituents: Octupolar Effect on Two-Photon Absorption. *Angew. Chem. Int. Ed.* **2008**, 47, 4840-4843.
14. a) Chen, Y; Chang, J; Lee, G; Wu, I; Fang, J; Wu, C; Pi, T. Enhancement in current efficiency in organic light-emitting diodes with incorporation of subphthalocyanine. *Appl. Phys. Lett.* **2009**, 95, 133302; b) Morse, G; Helander, M; Maka, J; Lu, Z; Bender, T. Fluorinated Phenoxy Boron Subphthalocyanines in Organic Light-Emitting Diodes. *ACS Appl. Mater. Interfaces*, **2010**, 2, 1934-1944.
15. a) Mutolo, K; Mayo, E; Rand, P; Forrest, S; Thompson, M. Enhanced Open-Circuit Voltage in Subphthalocyanine/C_{60} Organic Photovoltaic Cells. *J. Am. Chem. Soc.* **2006**, 128, 8108-8109; b) Beaumont, N; Cho, S; Sullivan, P; Newby, D; Smith, K; Jones, T. Boron Subphthalocyanine Chloride as an

Electron Acceptor for High-Voltage Fullerene-Free Organic *Photovoltaics. Adv. Funct. Mater.* **2012**, 22, 561-566.

16. a) Xue, Z; Mack, J; Lu, H; Zhang, L; You, X; Kuzuhara, D; Stillman, M; Yamada, H; Yamauchi, S; Kobayashi, N; Shen, Z. The Synthesis and Properties of Free-Base [14]Triphyrin(2.1.1) Compounds and the Formation of Subporphyrinoid Metal Complexes. *Chem. Eur. J.* **2011**, 17, 4396-4407; b) Kuzuhara, D; Yamada, H; Xue, Z; Okujima, T; Mori, S; Shen, Z; Uno, H. New synthesis of *meso*-free-[14]triphyrin(2.1.1) by McMurry coupling and its derivatization to Mn(I) and Re(I) complexes. *Chem. Commun.* **2011**, 47, 722-724.
17. a) L. Latos-Graz˙yn´ ski in The Porphyrin Handbook, Vol. 2 (Eds.: K. M. Kadish, K. M. Smith, R. Guilard), Academic Press, San Diego, **2000**, pp. 361-416 b) Chmielewski, P; Latos-Graz˙yn´ ski, L. Core modified porphyrins – a macrocyclic platform for organometallic chemistry. *Coord. Chem. Rev.* **2005**, 249, 2510-2533.
18. Kuzuhara, D; Yamada, H; Xue, Z; Okujima, T; Mori, S; Shen, Z; Uno, H. New synthesis of *meso*-free-[14]triphyrin(2.1.1) by McMurry coupling and its derivatization to Mn(I) and Re(I) complexes. *Chem. Commun*, **2011**, 47, 722-724.

Chapter 2: Crystallization and Physical Properties of Thiatripyrrine Co-crystal

2.1 Introduction

Intermolecular interactions are the basis for formation of co-crystals. Most intermolecular interactions such as Van der Waals interaction etc. are weak but a strong directional non-covalent force such as hydrogen bonding can act almost as much as covalent bonds and takes on new chemical and physical properties of its own in co-crystals. One of the prototypal examples of this type of co-crystal is quinhydrone, reported at least as early as 1844 [19] and 1893 [20]. This co-crystal was found to have a molar composition of 1:1 of parent compound of quinone and hydroquinone and formed by principle interaction of hydrogen bonding (figure 2.1).

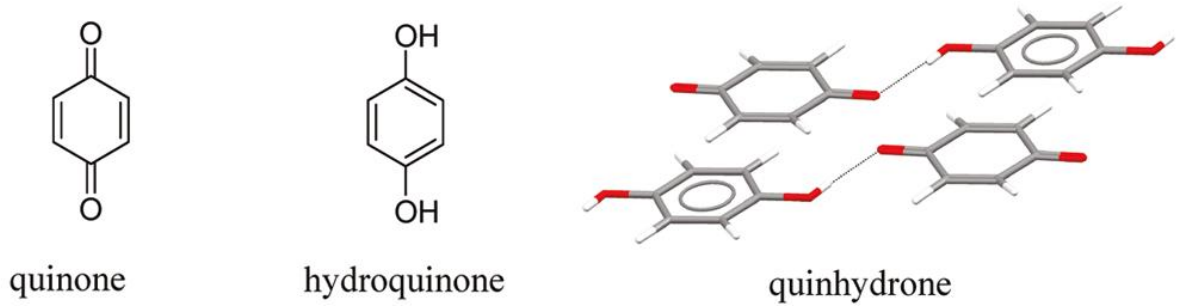

Figure 2.1: Chemical structures of quinine, hydroquinone and molecular structure of co-crystal quinhydrone

These types of co-crystals were continued to be discovered throughout 1900s, some of them by chance, others were the results of screening.

Hydrogen bonding can also be used to trap guest molecules having complementary hydrogen bonding site in the cavity of host molecules. Hamilton [22], Bell [23] and Reinhoudt [24] designed such types of complexes in which small gust molecules can be trapped in the cavity or at the surface of large host molecules. Recently Sessler and co-workers designed a molecule having U-shaped cavity which can trap benzene 'tweezers' and showed a remarkable change in the association features and optical properties having principle interaction of hydrogen bonding and other non-covalent interactions[25]. The concept could be applied to design a host molecule composed of multiple hydrogen bonded subunits forming a U-shaped cavity which can trap small guest molecules having complementary hydrogen bonding sites.

The definition of co-crystals remains a matter of discussion in the crystallography field to date. A useful modern definition of co-crystals, provided by Stahly [21] is that

“Co-crystals consists of two or more components that form a unique crystalline structure having unique properties”.

In this chapter of the thesis work, Thiatripyrrine **4**, a semi-solid compound (in its pure form) was used as a host molecule, co-crystallized with guest molecules dimethylformamide (DMF), acetone and acetonitrle (liquids in their pure form). Since this thiatripyrrine have two pyrrole NH groups which can act as good hydrogen-bond donor from both the sides making it good molecule candidate for co-crystal formation and carbonyl group (=O) of DMF and acetone, nitrile group (-CN) of acetonitrile can act as a good hydrogen-bond acceptor (figure 2.2).

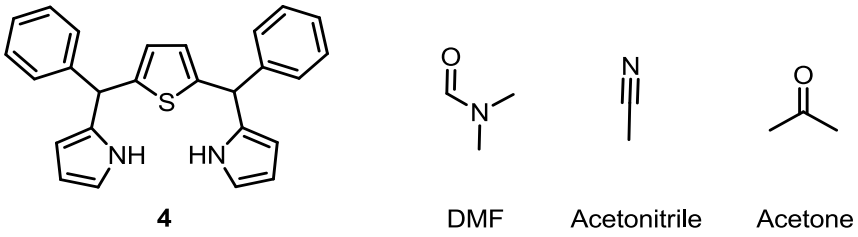

Figure 2.2: Chemical structures of thiatripyrrine (**4**), DMF, Acetonitrile and Acetone

There are multitude synthetic strategies that are available in the literature to synthesize co-crystals. These include evaporation of a heteromeric solution, solid state grinding, kneading, sublimation, growth from the melt, reaction crystallization, and slurry preparation etc [26].

In this chapter of thesis work, co-crystals were grown by dissolving one parent compound into the other parent compound which acts as a solvent and passing the resulting solution through the syringe or cannula resulted in the immediate nucleation of co-crystals suitable for single crystal X-ray diffraction which is a unique method of preparation of co-crystals to date.

2.2 Preparation, Results and Discussion

The thiatripyrrine **4** (a semi-solid compound) was synthesized as reported in the chapter 1 and characterized by ^{1}H NMR, HRMS (refer to chapter 1) and single crystal XRD. In a round bottom flask of 100 ml, 8 g of thiatripyrrine was dissolved in 70 ml of DMF and argon was bubbled through it. The 10 ml of resulting yellowish colour solution was taken into a 10 ml syringe. The yellowish colour of the solution in syringe immediately changed to black colour. Upon mixing with the parent yellowish solution, the whole solution in the round bottom flask changed to black colour and resulted in large single crystals within 2-3 minutes. This black solution containing crystals was filtered separated for further analysis.

The same process was employed for thiatripyrrine with acetone and acetonitrile. The rate of formation of crystals was found to be highest in case of DMF and lowest for acetone.

2.2.1 Thaitripyrrine – DMF co-crystal

The obtained crystals were analyzed by single crystal XRD and could be identified as 1:1 thiatripyrrine : DMF co-crystals, with the space group C m, cell lengths a = 5.8577 Å, b = 21.418 Å, c = 9.568 Å. Figure 2.3 shows the packing diagram.

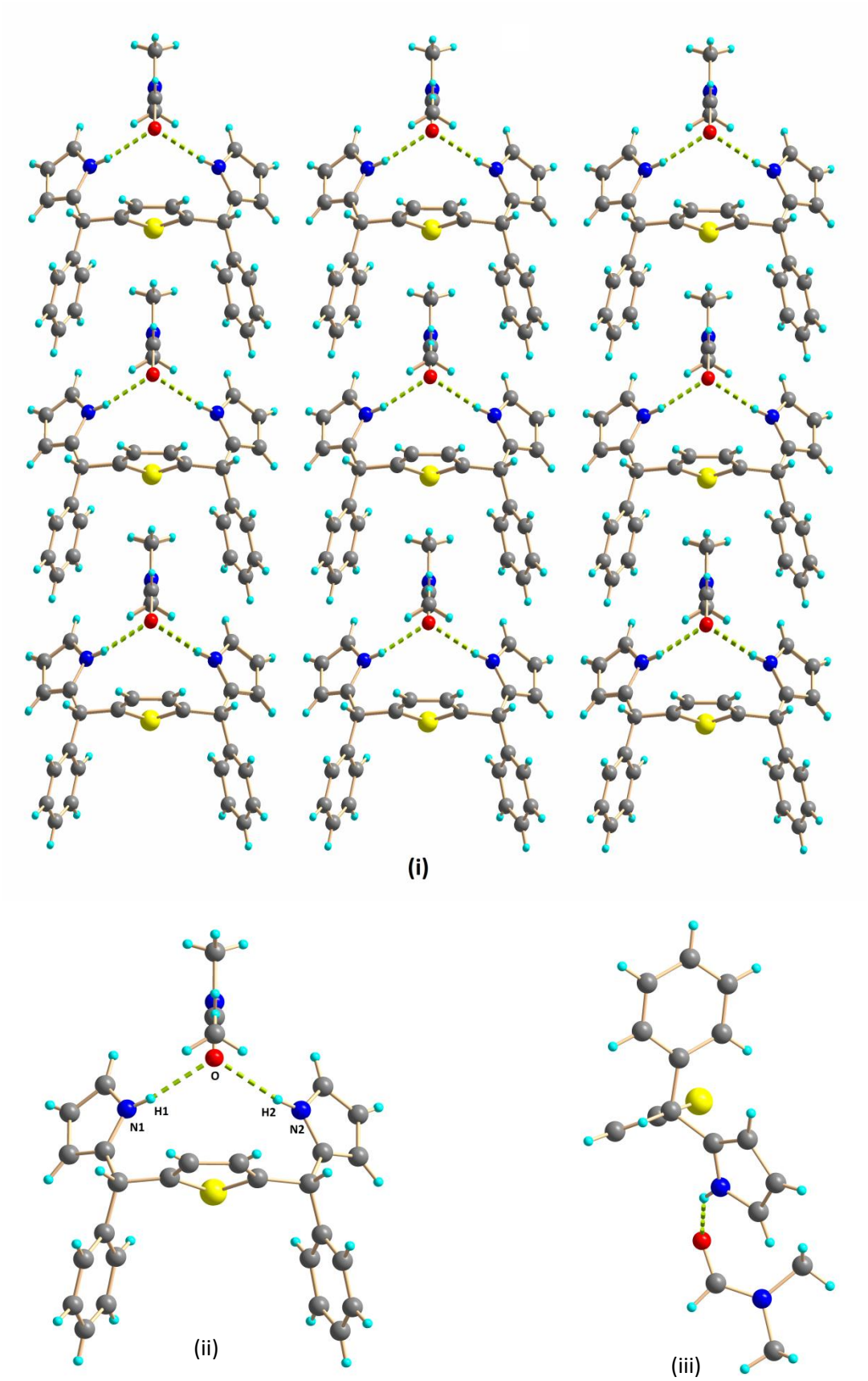

Figure 2.3: Packing diagram of (i) thiatripyrrine-DMF co-crystal, (ii) down the 'a' axis, (iii) down the 'b' axis

Thiatripyrrine and DMF are connected by O···H hydrogen bonds between the oxygen atom of DMF and the nitrogen atom of thiatripyrrine. The hydrogen bonding distance and angle are listed in table 2.1.

D-H···A	D-H (Å)	H···A (Å)	D···A (Å)	D-H···A (°)
N1-H1···O	0.861	2.161	2.931	148.70
N2-H2···O	0.861	2.161	2.931	148.70

Table 2.1: Hydrogen bond geometry in thiatripyrrine-DMF co-crystal

The IR spectrum of thiatripyrrine-DMF co-crystal is shown in Figure 2.4. Particular change in the frequency was observed around 1500 – 1700 cm^{-1}. The presence of peak at 1649 cm^{-1} shows the DMF in the co-crystal. The reduction in frequency by 57 cm^{-1} shows that –C=O is hydrogen bonded as –C=O frequency in DMF is reported as 1707 cm^{-1} [27].

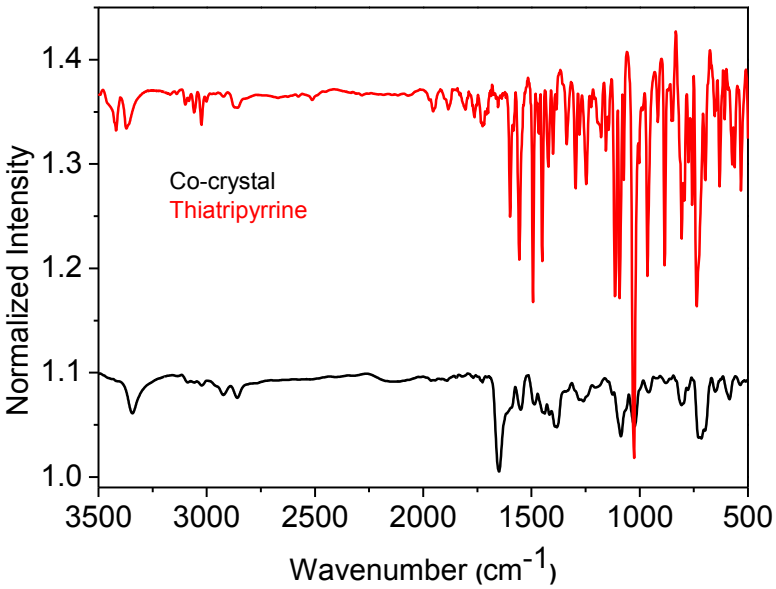

Figure 2.4: FTIR spectra of the 1:1 thiatripyrrine : DMF co-crystal

Thermal analysis of thiatripyrrine-DMF co-crystal was done by TGA. Melting point of the co-crystal was found to be 116° C which is lower than the melting point of crystalline thiatripyrrine (123° C).

Figure 2.5 is the TGA result of thiatripyrrine-DMF co-crystals. At 170° C the weight has decreased to about 80% of the initial sample weight and there is clear change in the slope of curve. Considering the co-crystal composition as 1:1 of thiatripyrrine to

DMF (the molar mass of thiatripyrrine 394.15 g/mol and the molar mass of DMF 73.05 g/mol), 18.5% of the co-crystal weight corresponds to the amount of DMF. This tells us that co-crystal disintegrates over the temperature range 100 - 170° C. So we may conclude based on its melting temperature and TGA disintegration temperature range that decomposition of co-crystals takes place around 116° C.

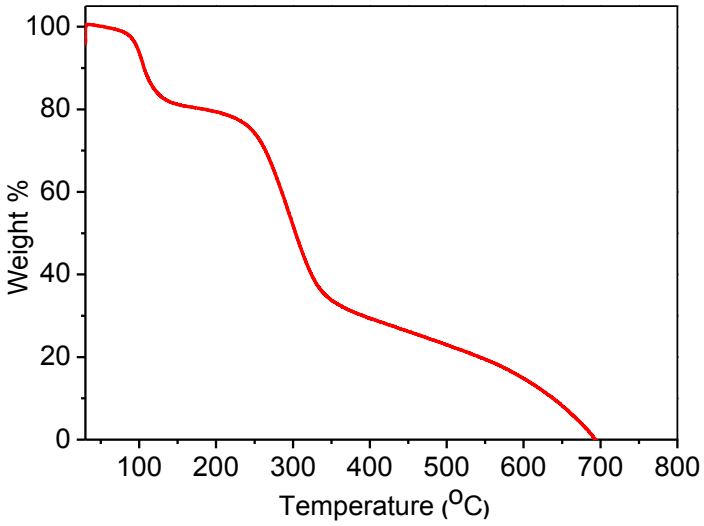

Figure 2.5: TGA graph of the 1:1 thiatripyrrine : DMF co-crystal

Figure 2.6 shows the UV-Visible spectra of thiatripyrrine-DMF co-crystal in DCM, $CHCl_3$ and ethyl acetate solvents. The free thiatripyrrine absorbs at 473 nm whereas thiatripyrrine-DMF co-crystals weakly absorbs in DCM and $CHCl_3$ as shown in Figure 2.6. In ethyl acetate solvent, thiatripyrrine-DMF co-crystals were found to achieve the free thiatripyrrine absorbance with the passage of time. We may conclude that in ethyl acetate solvent, free thiatriphyrin reverts back to its initial conformation as shown in Figure 2.7(i).

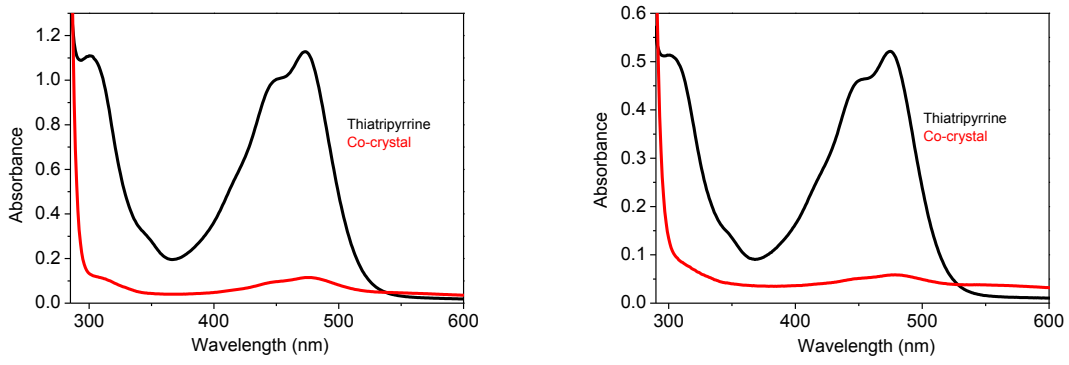

(i) (ii)

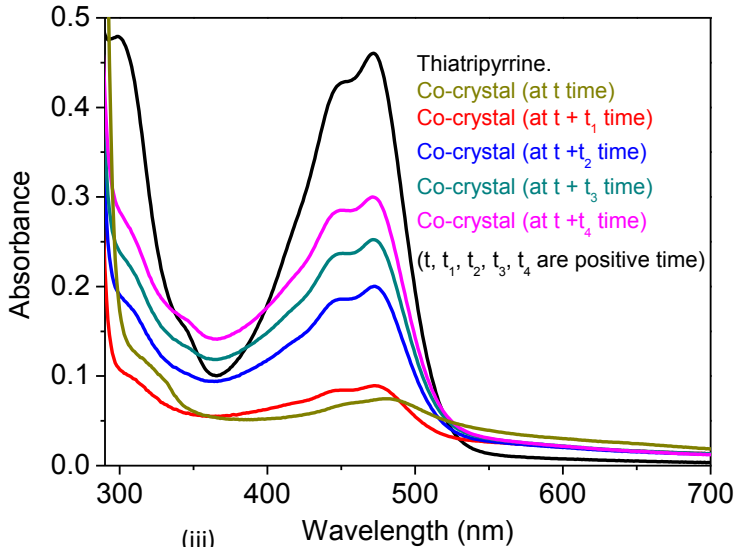

Figure 2.6: UV-Visible spectra of thiatripyrrine-DMF co-crystal in (i) DCM, (ii) CHCl3 and (iii) Ethyl acetate

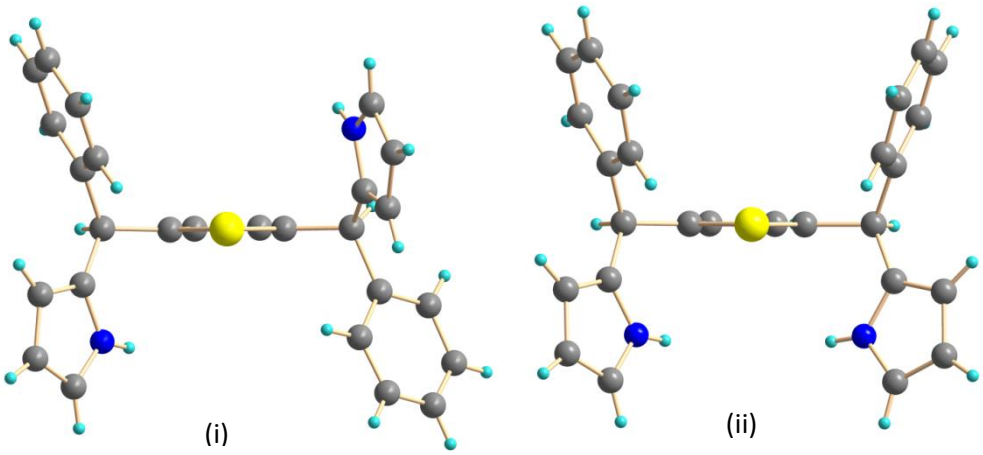

Figure 2.7: (i) conformation of free thiatripyrrine, (ii) conformation of thiatripyrrine in co-crystal

2.2.2 Thaitripyrrine – Acetonitrile co-crystal

Similar to the above co-crystal, single crystal XRD identifies the co-crystals as 1:1 thiatripyrrine : Acetonitrile co-crystals, with the space group C m, cell lengths a = 5.7039 Å, b = 21.124 Å, c = 9.5885 Å. Figure 2.8 shows the packing diagram.

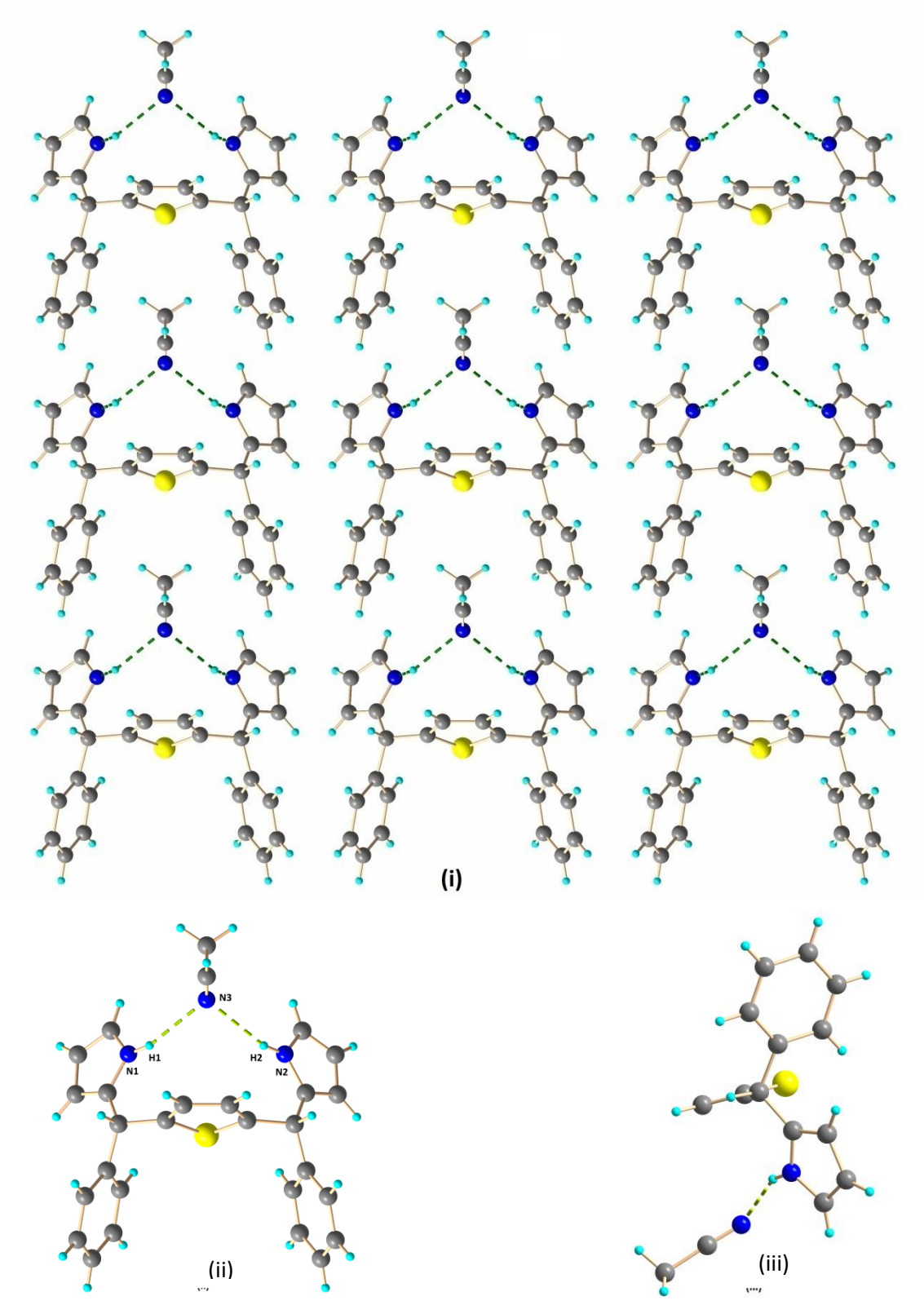

Figure 2.8: Packing diagram of (i) thiatripyrrine-Acetonitrile co-crystal, (ii) down the 'a' axis, (iii) down the 'b' axis

Thiatripyrrine and Acetonitrile are connected by N···H hydrogen bonds between the nitrogen atom of acetonitrile and the nitrogen atom of thiatripyrrine. The hydrogen bonding distance and angle are listed in table 2.2.

D-H···A	D-H (Å)	H···A (Å)	D···A (Å)	D-H···A (°)
N1-H1···N3	0.859	2.372	3.179	156.87
N2-H2···N3	0.859	2.372	3.179	156.87

Table 2.2: Hydrogen bond geometry in thiatripyrrine-acetonitrile co-crystal

The IR spectrum of thiatripyrrine-Acetonitrile co-crystal is shown in Figure 2.9. Particular change in the frequency was observed around 2100 – 2500 cm^{-1}. The presence of peak at 2247 cm^{-1} shows the acetonitrile in the co-crystal and the reduction in frequency by 33 cm^{-1} shows that –CN is hyndrogen bonded as –CN frequency in DMF is reported as 2280 cm^{-1} [28].

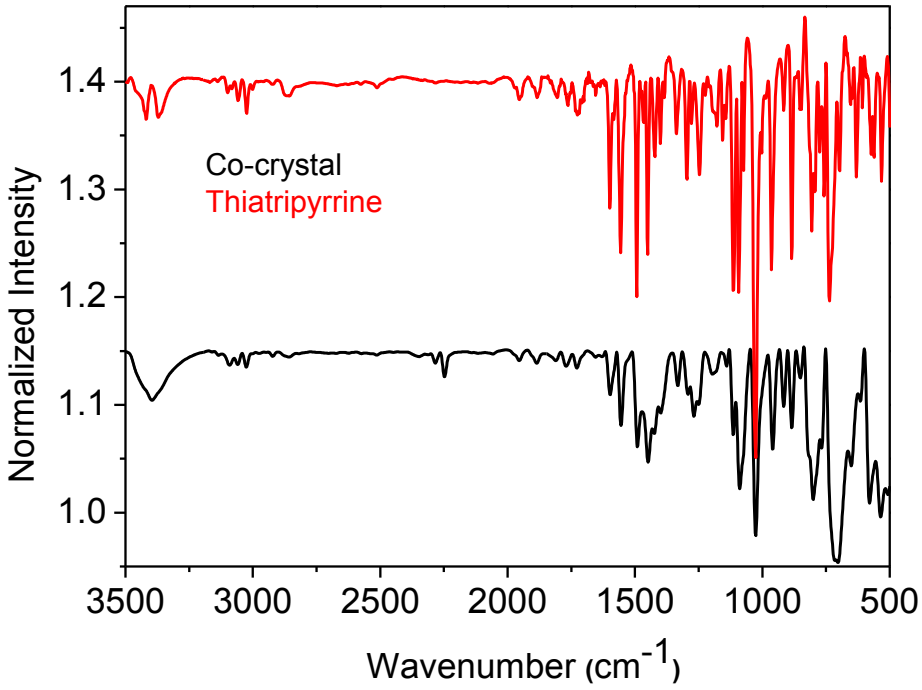

Figure 2.9: FTIR spectra of the 1:1 thiatripyrrine : acetonitrile co-crystal

Melting point of the co-crystal was found to be 86° C. Figure 2.10 is the TGA result of thiatripyrrine-acetonitrile co-crystals. At 147°C the weight decreased to about 93% of the initial sample weight and there is clear change in the slope of curve. Considering the co-crystal composition as 1:1 of thiatripyrrine to acetonitrile (the molar mass of

thiatripyrrine 394.15 g/mol and the molar mass of Acetonitrile 41.02 g/mol), 10.4% of the co-crystal weight corresponds to the amount of Acetonitrile. This tells us that co-crystal disintegrates over the temperature range 60 - 147° C. So we may conclude based on its melting temperature and TGA disintegration temperature range that decomposition of co-crystals takes place around 86° C.

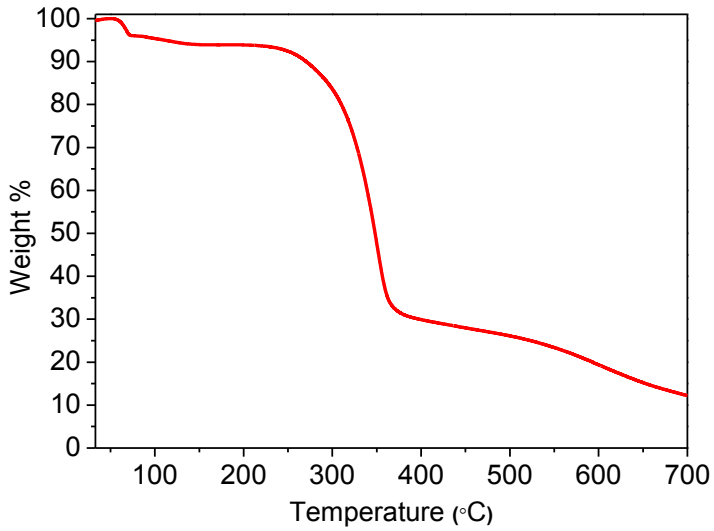

Figure 2.10: TGA graph of the 1:1 thiatripyrrine : Acetonitrile co-crystal

2.2.3 Thaitripyrrine – Acetone co-crystal

Similar to the above both co-crystal, Single crystal XRD identifies the co-crystals as 1:1 thiatripyrrine : acetone co-crystals, with the space group C m, cell lengths a = 5.7039 Å, b = 21.124 Å, c = 9.5885 Å. Figure 2.11 shows the packing diagram.

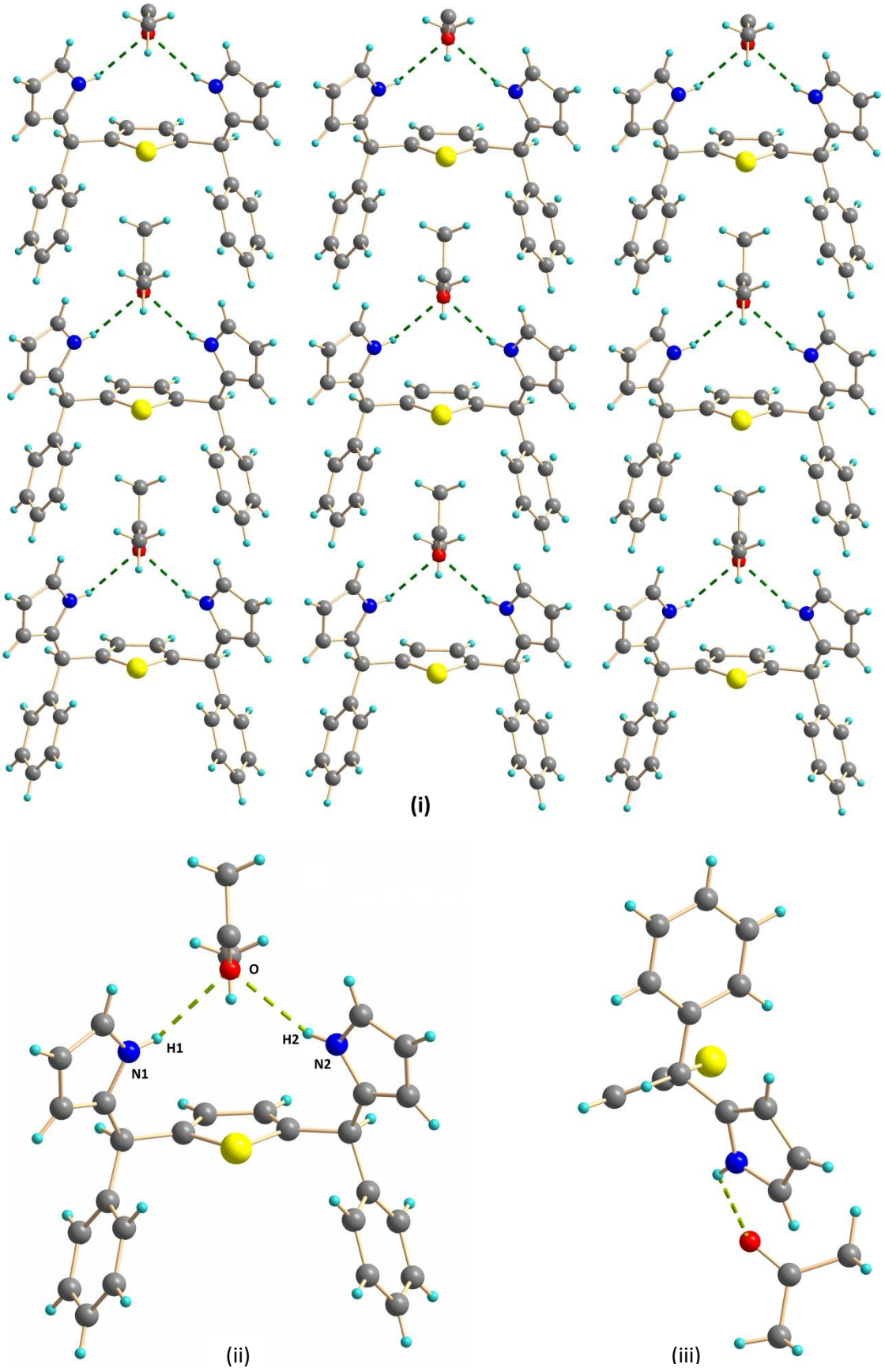

Figure 2.11: Packing diagram of (i) thiatripyrrine-acetone co-crystal, (ii) down the 'a' axis, (iii) down the 'b' axis

Thiatripyrrine and acetone are connected by O···H hydrogen bonds between the oxygen atom of acetone and the nitrogen atom of thiatripyrrine. The hydrogen bonding distance and angle are listed in table 2.3.

D-H···A	D-H (Å)	H···A (Å)	D···A (Å)	D-H···A (°)
N1-H1···O	0.860	2.524	3.131	128.33
N2-H2···O	0.860	2.524	3.131	128.33

Table 2.3: Hydrogen bond geometry in thiatripyrrine-acetone co-crystal

The IR spectrum of thiatripyrrine-acetone co-crystal is shown in Figure 2.12. Particular change in the frequency was observed around 1500 – 1800 cm^{-1}. The presence of peak at 1693.54 cm^{-1} shows the acetone in the co-crystal and the reduction in frequency by 21.46 cm^{-1} shows that –C=O is hydrogen bonded as –C=O frequency in acetone is reported as 1715 cm^{-1} [29].

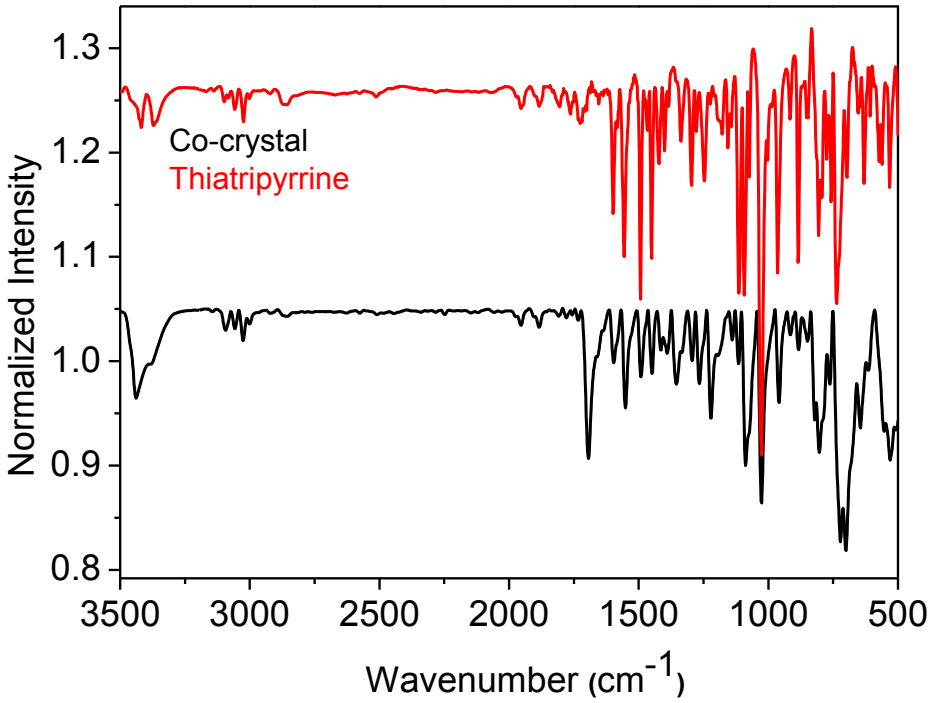

Figure 2.12: FTIR spectra of the 1:1 thiatripyrrine : Acetone co-crystal

Melting point of the co-crystal was found to be 73° C. Figure 2.13 is the TGA result of thiatripyrrine-acetone co-crystals. At 140° C the weight decreased to about 89% of the initial sample weight. Considering the co-crystal composition as 1:1 of thiatripyrrine to Acetone (the molar mass of thiatripyrrine 394.15 g/mol and the molar

mass of Acetone 58.04 g/mol), 14.7% of the co-crystal weight corresponds to the amount of Acetone. This tells us that co-crystal disintegrates over the temperature range 54 - 140° C. So we may conclude based on its melting temperature and TGA disintegration temperature range that decomposition of co-crystals takes place around 73° C.

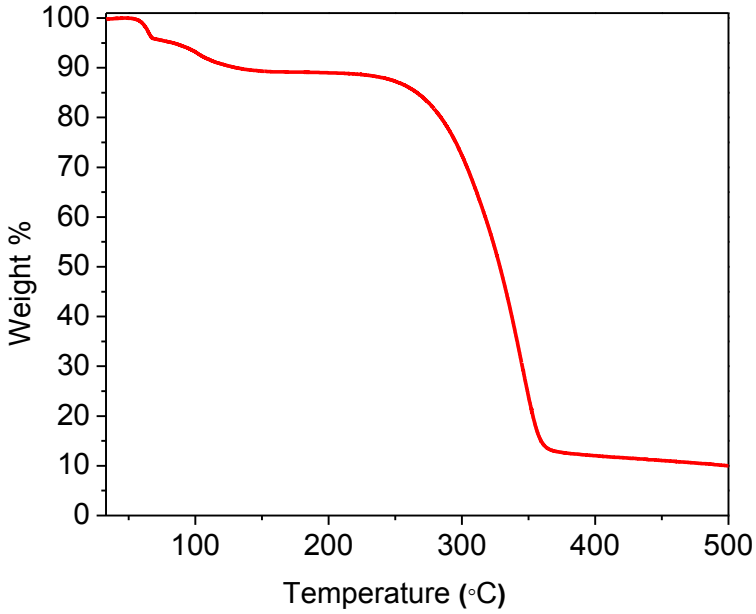

Figure 2.13: TGA graph of the 1:1 thiatripyrrine : Acetone co-crystal

The crystalline array of these resulted co-crystals composed of a host semi-solid compound and a guest liquid compound under ambient conditions in their pure form were found to be stabilized by principle interaction of hydrogen bonding. The formation of hydrogen bonding was confirmed by examining the corresponding distances among donor, acceptor and hydrogen with the geometrical criteria of hydrogen bonding {as main three empirical rules for hydrogen bonding were proposed [30]; rule 1) donor-acceptor distance (D-A) < 3.9Å, rule 2) hydrogen-acceptor distance (H-A) < 2.5Å, rule 3) angle between donor-hydrogen-acceptor (D-H-A) > 90°}.

By looking at their respective hydrogen-acceptor (H···A) distances, their disintegration temperatures, the differences in their IR values, the stability of the co-crystals were concluded as;

$$\text{Co-crystal}_{(\text{thiatripyrrine-DMF})} > \text{Co-crystal}_{(\text{thiatripyrrine-acetonitrile})} > \text{Co-crystal}_{(\text{thiatripyrrine-acetone})}$$

	Dimethylformamide (DMF)	Acetonitrile	Acetone	Thiatripyrrine (Thtripy)
Moiety formula	Thtripy·DMF	Thtripy·CH_3CN	Thtripy·C_3H_6O	Thtripy
Chemical formula	$C_{29}H_{29}N_3OS$	$C_{28}H_{25}N_3S$	$C_{29}H_{28}N_2OS$	$C_{26}H_{22}N_2S$
M (g mol^{-1})	467.20	435.18	452.19	394.15
T (K)	100	100	100	100
Crystal System	Monoclinic	Monoclinic	Monoclinic	Monoclinic
Space group	Cm	Cm	Cm	$P2_1/n$
a (Å)	5.8577(19)	5.7039(9)	5.7742(12)	5.929(3)
b (Å)	21.418(6)	21.124(3)	21.733(5)	13.162(8)
c (Å)	9.568(3)	9.5885(15)	9.456(2)	26.290(15)
α (°)	90.00	90.00	90.00	90
β (°)	97.158(8)	98.592(3)	98.461(4)	94.343(15)
γ (°)	90.00	90.00	90.00	90
V ($Å^3$)	1191.05	1142.34	1173.72	2045.71
Z/Z'	2/0	2/0	2/0	4/0
R1	0.0514	0.0318	0.0394	0.0773

Table 2.4: Crystallographic data for thiatripyrrine co-crystals

We also attempted to form co-crystals of thiatripyrrine with DMSO, $POCl_3$ and nitromethane. Co-crystals obtained from DMSO were found to be unstable under ambient conditions as these co-crystals changed into black color from colorless co-crystals with the passage of time. The characterization of such unstable co-crystals is in process. Co-crystallization of thiatripyrrine with $POCl_3$ and nitromethane was unsuccessful as color of the yellowish solution changed into black immediately after addition of nitromethane and $POCl_3$.

Selective hydrogen bonding appears to be the prime reason for the formation of these co-crystals due to the optimized distance between two pyrrole moieties. To check this plausible reason, we tried to form the same with 2,2'-(phenylmethylene)bis(1H-pyrrole) which lack thiophene moiety between two pyrrole

moieties and 5,5'-bis(phenyl(1H-pyrrol-2-yl)methyl)-2,2'-bithiophene which has two thiophene moieties between two pyrrole moieties (Figure 2.14).

2,2'-(phenylmethylene)bis(1*H*-pyrrole) **10**

5,5'-bis(phenyl(1*H*-pyrrol-2-yl)methyl)-2,2'-bithiophene **11**

Figure 2.14: Chemical structures of 2,2'-(phenylmethylene)bis(1H-pyrrole) and 5,5'-bis(phenyl(1H-pyrrol-2-yl)methyl)-2,2'-bithiophene

These both the compounds were not found to form co-crystals with any of the above mentioned molecules (DMF, Acetonitrile, Acetone). This could be explained by the distances between two pyrrole moieties which doesn`t match to form hydrogen bond. Their solid state crystal structures obtained are shown in Figure 2.15.

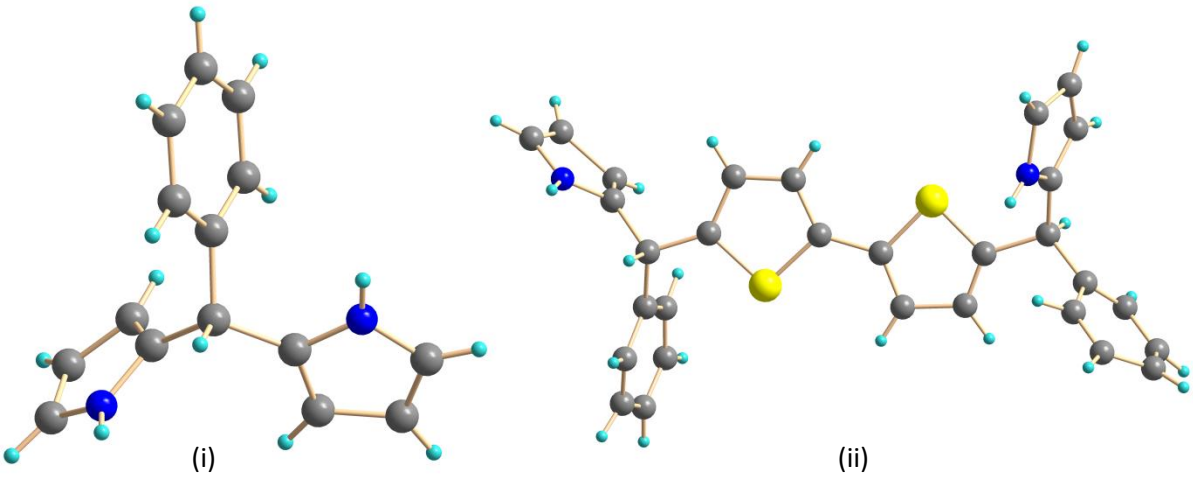

Figure 2.15: Crystal structures of (i) 2,2'-(phenylmethylene)bis(1H-pyrrole), (ii) 5,5'-bis(phenyl(1H-pyrrol-2-yl)methyl)-2,2'-bithiophene

We estimated the energy required for a free thiatripyrrine to change its conformation. The energy profile of its alternate conformation is shown in figure 2.16. The minimum energy corresponds to the free thiatripyrrine with total energy (Hartree) = -1511.71048085 whereas thiatripyrrine conformation's (in co-crystals) total energy was found to be -1511.70922459 Hartree. This suggests that both the conformations are well stabilized compared to its other conformation separated by a conformation energy barrier.

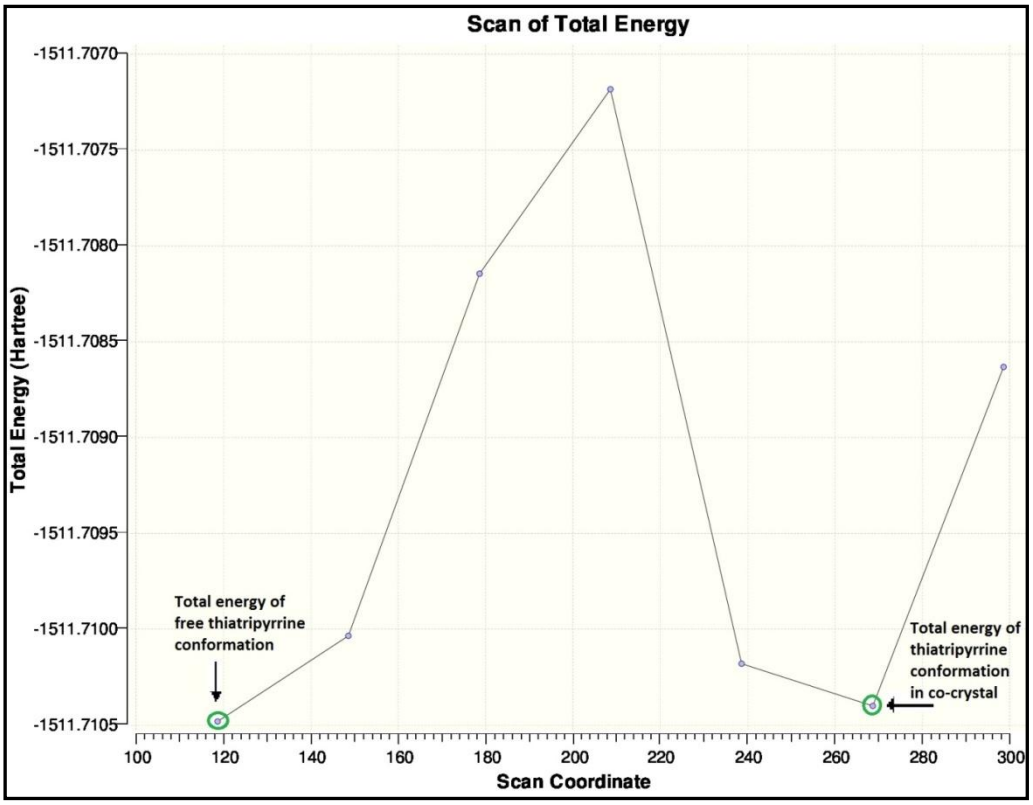

Figure 2.16: Total energy profile of thiatripyrrine conformations

This suggests that in order to form hydrogen bonding, thiatripyrrine has to cross a conformation energy barrier and this required energy is probably given by the passing these molecules from the open volume to a confined volume and back to the open volume and also by its thermodynamic stability because of hydrogen bonding after forming co-crystals.

Density functional theory (DFT) with Becke`s three-parameter hybrid exchange functional and the Lee-Yang-Parr correlation functional (B3LYP) and 6-31G(d,p) basis set for all the atoms were employed in the calculations. The molecular structure of free thiatripyrrine obtained from single crystal analysis was used to obtain the geometry optimized structures. Optimization was done along the dihedral angle (as shown in figure 2.17) each by 30° from 118.6366 to -64.3634.

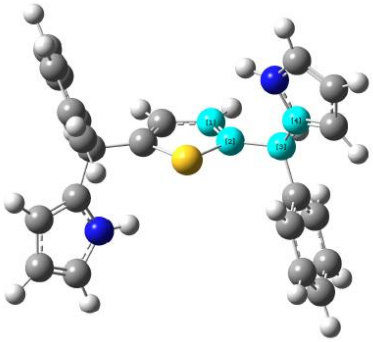

Figure 2.17: Optimized geometry of free tripyrrine showing dihedral angle

Compound **11** was synthesized using following scheme;

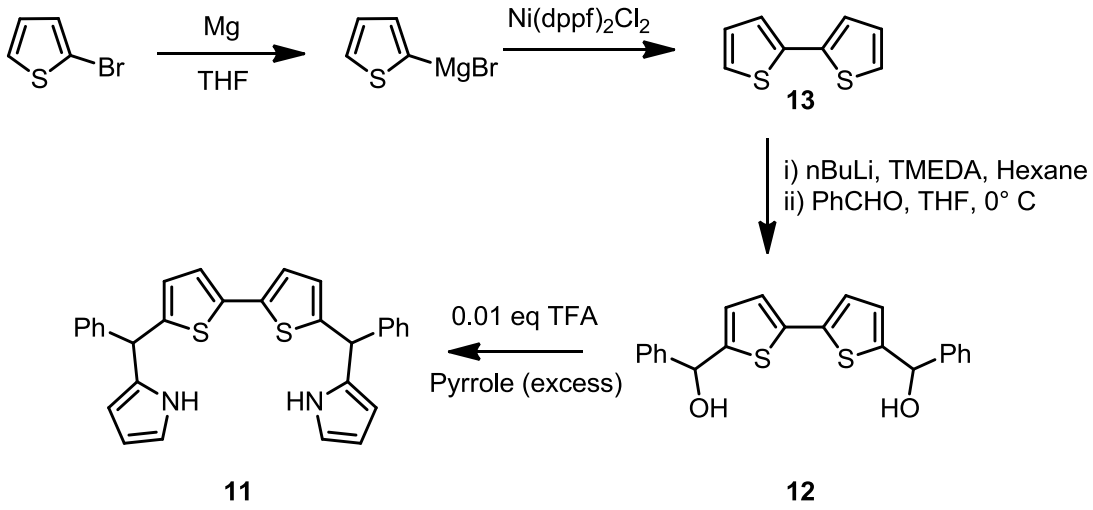

Figure 2.18: Synthetic scheme of compound **11**

2.3 Summary

In this chapter of our study, we have identified the co-crystals of thiatripyrrine with a unique method of preparation. These co-crystals are having a parent component of semi-solid and other liquid component. All the co-crystals were relatively stable and the order of thermal stability (Co-crystal $_{(DMF)}$ > Co-crystal $_{(acetonitrile)}$ > Co-crystal $_{(acetone)}$) follows the order of boiling points of entrapped molecules. These molecules are located at the specific site within the structure stabilized by principle interaction of hydrogen bonding. There is also a change in the conformation of thiatripyrrine in the co-crystals compared to its free conformation which suggests that this multi-component system is thermodynamically stable with principle interaction of hydrogen bonding. This indicates the destruction of original thiatripyrrine structure followed by a complex reorganization process. Computational studies reveal the stabilization of

both the conformations separated by a conformation energy barrier. These conformations were found to be reversible.

2.4 Experimental Methods

2.4.1 Chemicals for Synthesis:

Common solvents used for synthesis were purified and dried according to known procedures. 2-Bromothiophene, TMEDA were used from Alrich chemicals, USA. Pyrrole, TFA and benzaldehyde were used from Spectrochem chemicals. Pyrrole and benzaldehyde were distilled before use. n-Butyllithium (1.6M in hexane) was used from E. Merck, Germany. Anhydrous potassium carbonate, anhydrous sodium sulphate, and anhydrous calcium chloride were obtained from Rankem Fine chemicals, India.

2.4.2 Synthesis of Chemical Compounds

2,2'-(phenylmethylene)bis(1H-pyrrole) (10)

Benzaldehyde (2 ml, 0.0196 mol) was dissolved in excess of pyrrole (67.9 ml) and argon was bubbled through it. Trifloroacetic acid (TFA) (0.15 ml, 0.002 mol) was added and the resulting mixture was allowed to stir for 1 hr. The reaction was stopped by addition of DCM (50 ml) followed by 40% NaOH (15 ml). The organic layer was separated and washed with water and brine, dried over Na_2SO_4 and concentrated under reduced pressure. The desired compound was separated via column chromatography on silica gel.

^{1}H NMR (400 MHz, $CDCl_3$) δ 7.94 (brs, 2 NH), δ 7.35 – 7.23 (m, 5H), δ 6.71 (m, 2H), δ 6.19 (m, 2H), δ 5.94 (m, 2H), δ 5.49 (s, 1H) Crystallographic data: $C_{15}H_{14}N_2$, M = 222.16, monoclinic, space group $P2_1/n$, a = 5.8781(14), b = 17.957(4), c = 11.683(3), α = 90°, β = 98.118(6)°, γ = 90°, V = 1220.82 Å^3, Z = 4, R = 0.043.

2,2'-bithiophene (13)

Activated Mg (0.75 gm,31 mmol) was added to dry THF (30 ml) followed by a pinch of iodine. The resulting mixture was stirred for 5-10 minutes and color of solution changed to light brown. Then 2-bromo thiophene (3 ml, 31 mmol) was added slowly and after some time solution became colorless. Vigorous bubbling was observed and color changed to dark brown. 2-bromo thiophene (2.5 ml, 25.8 mmol) was added slowly at 0° C and temperature was maintained. $Ni(dpp)_2Cl_2$ was added slowly to the

reaction mixture. The solution mixture was brought to room temperature and was refluxed at 90° C for 3 hrs. The reaction was quenched with dil. HCl while keeping it in ice bath. The organic layer was separated and washed with water and dried over sodium sulpahte, concentrated under reduced pressure. The desire product was obtained as colorless viscous liquid. (Yield: 80%) [31]

^{1}H NMR (400 MHz, $CDCl_3$) δ 7.20 (d, 2H), δ 7.17 (d, 2H), δ 7.00 (dd, 2H)

[2,2'-bithiophene]-5,5'-diylbis(phenylmethanol) (12)

Compound **13** (2.5 gm, 15.06 mmol) was added slowly via a syringe to a solution of n-BuLi (29.86 ml of 1.6M solution in hexane) and tetramethylethylenediamine (TMEDA) (7.0 ml) in 100 ml of dry hexane under an argon atmosphere. The resulting solution was warmed and then refluxed for 1 hr, and then cooled to ambient temperature. This dilithiothiophene solution was added slowly to a solution of benzaldehyde (4.00 ml, 57.65 mmol) in dry THF cooled to 0° C in an ice bath. The ice bath was removed after addition and the reaction was warmed to ambient temperature. The reaction was quenched by a cold, saturated NH_4Cl solution (200 ml) and the organic layer was separated, dried over Na_2SO_4 and concentrated under reduced pressure. The desired compound was isolated via column chromatography on silica gel eluted with ethyl acetate/hexane. (Yield: 80%)

^{1}H NMR (400 MHz, $CDCl_3$) δ 7.44 – 7.30 (m, 10H), δ 6.90 (d, J = 4Hz, 2H), δ 6.73 (d, J = 4Hz, 2H), δ 5.97 (s, 2H), δ 2.40 (brs, OH)

5,5'-bis(phenyl(1H-pyrrol-2-yl)methyl)-2,2'-bithiophene (11)

Compound **12** (1.45 g, 3.05 mmol) was dissolved in excess pyrrole (11.01 ml) and argon was bubbled through it. CF_3COOH (0.03 ml) was added and the resulting mixture was allowed to stir for 1 hr. The reaction was quenched by the addition of dichloromethane (60 ml) followed by 40% NaOH (20 ml). The organic layer was separated, washed with water and brine, dried over sodium sulphate and concentrated under reduced pressure. The residual oil was purified via chromatography on silica gel eluted with ethyl acetate/hexane. (Yield: 90%)

^{1}H NMR (400 MHz, $CDCl_3$) δ 7.90 (brs, 2NH), δ 7.33 – 7.24 (m, 10H), δ 6.88 (d, J = 4Hz, 2H), δ 6.69 (m, 2H), δ 6.64 (d, J = 4Hz, 2H), δ 6.14 (m, 2H), δ 5.94 (m, 2H), δ 5.58 (s, 2H).

Crystallographic data: $C_{30}H_{24}N_2S_2$, M = 476.14, monoclinic, space group C c, a = 17.408(5), b = 5.5052(16), c = 25.524(7), α = 90°, β = 105.912(5)°, γ = 90°, V = 2352.36 Å^3, Z = 4, R1 = 0.0569.

2.5 Characterization spectral data:

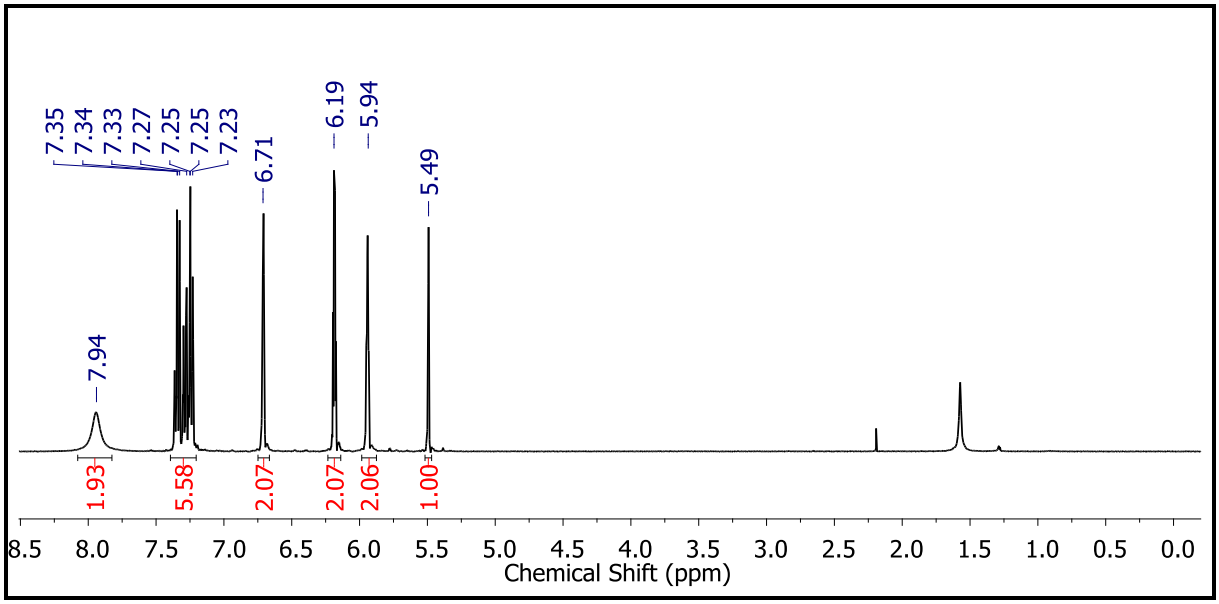

Figure 2.19: ^{1}H NMR of **10**

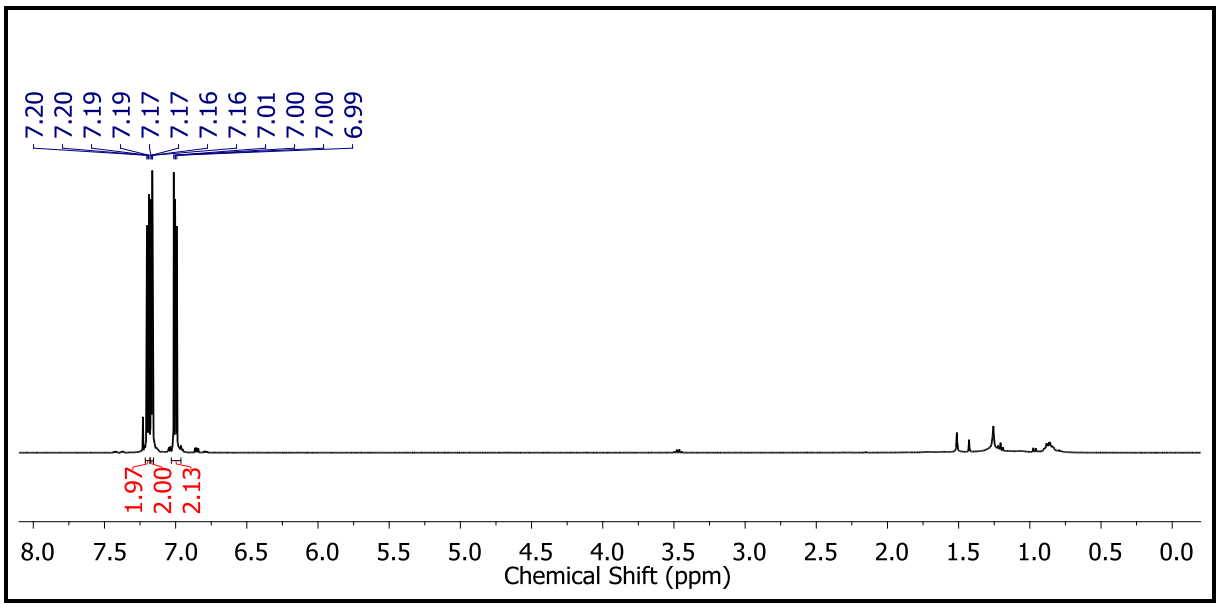

Figure 2.20: ^{1}H NMR of **13**

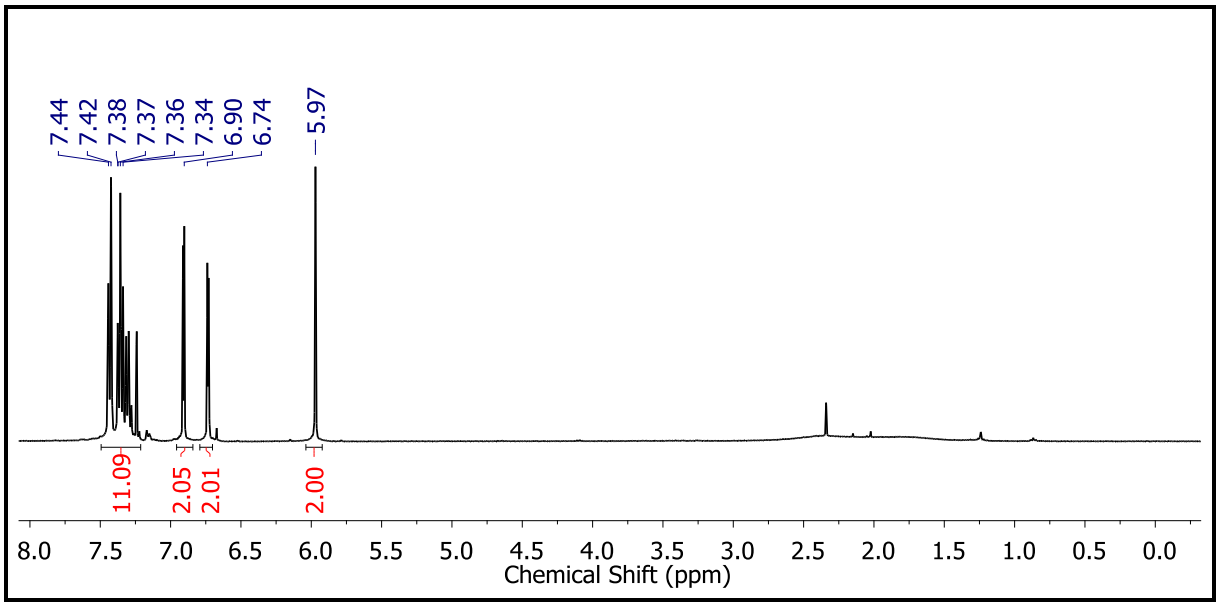

Figure 2.21: ^{1}H NMR of **12**

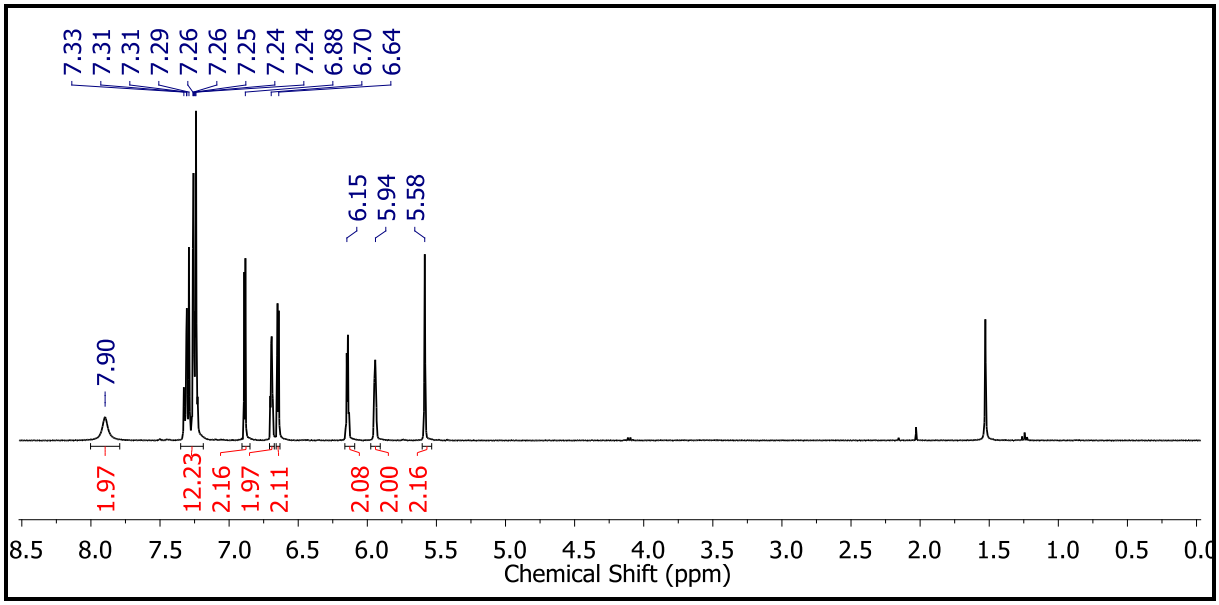

Figure 2.22: ^{1}H NMR of **11**

2.6 References

19. Wo¨hler, F; Untersuchungen u¨ ber das chinon.Annalen. **1844**, 51,153.
20. Ling, R; Baker L. Halogen derivatives of quinone Part III. Derivatives of quinhydrone. *J Chem Soc*, **1893**, 63, 1314–1327.
21. Stahly, G. Diversity in Single- and Multiple-Component Crystals. The Search for and Prevalence of Polymorphs and Cocrystals. *Cryst. Growth Des*., **2007**, 7, 1007.
22. Hamilton, A. D.; Van Engen, D. Induced fit in synthetic receptors: nucleotide base recognition by a molecular hinge. *J. Am. Chem. Soc.* **1987**, 109, 5035 - 5038.
23. Bell, T. W.; Liu, J. Hexagonal Lattice Hosts for Urea. A New Series of Designed Heterocyclic Receptors. *J. Am. Chem. Soc.* **1988**, 110, 3673-3674.
24. Van Stavern, C. J.; Fenton, D. E.; Reinhoudt, D. N.; Van Erden, J.; Harkema, S. Complexes of crown ethers and neutral molecules; synthesis and crystal structure of a urea 18-crown-6(5 : 1) complex. *J. Chem. Soc., Chem. Commun.* **1981**, 368.

25. Kim, S; Lim, J; Pradhan, T; Jung, H; Lynch, V; Kim, J; Kim, D; Sessler, J. Self-Association and Nitroaromatic-Induced Deaggregation of Pyrene Substituted Pyridine Amides. *J. Am. Chem. Soc.* **2014**, 136, 495−505.
26. Blagden, N; Berry, D; Parkin, A; Ibrahim, H; Gavan, P; Matos L; Seaton C. Current directions in co-crystal growth. *New J. Chem.,* **2008**, 32, 1659–1672.
27. Park, S; Min, K; Lee, C; Hong, S; Kim, Y; Lee, N. Intermolecular Hydrogen Bonding and Vibrational Analysis of N,N-Dimethylformamide Hexamer Cluster. Bull. *Korean Chem. Soc.* **2009**, 30, 11, 2595-2602.
28. http://wpscms.pearsoncmg.com/au_hss_brown_chemistry_1/57/14650/3750498.cw/-/3750521/index.html
29. http://www.mhhe.com/physsci/chemistry/carey/student/olc/graphics/carey04oc/ref/ch13ir.html
30. Torshin, I; Weber, I; Harrison, R. Geometric criteria of hydrogen bonds in proteins and identification of "bifurcated" hydrogen bonds. *Protein Engineering*, **2002**, 15, 5, 359-363.
31. Yu, J; Shen, T; Weng, W; Huang, Y; Huang, C; Su, W; Rwei, S; Ho, K; Wang, L. Molecular Design of Interfacial Modifiers for Polymer-Inorganic Hybrid Solar Cells. *Adv. Energy Mater.* **2012**, 2, 245–252.